EC-Earth3 oceanographic analysis: Temperature increase in the Western Ross Sea explained

MSc thesis

Author: Amadi Ali, S. (Sophie)
Student number: 5850444
Email: s.amadiali@students.uu.nl

26-04-2023

Koninklijk Nederlands
Meteorologisch Instituut
Ministerie van Infrastructuur en Waterstaat

Utrecht University

Supervisor & first corrector:
Sybren Drijfhout

Supervisors:
Eveline van der Linden
Erwin Lambert
Claire Donnelly

Second corrector:
Roderik van de Wal

ABSTRACT

The Ross Sea plays a role in the global overturning circulation, is one of the largest CO2 sinks of Antarctica, and has a large influence on the Antarctic Ice Sheet. The stability of this sheet has great influence on sea level rise, experienced all over the world.
In an idealized meltwater perturbation experiment around Antarctica with a time span of 150 years in the EC-Earth3 climate model, the Western Ross Sea ocean temperatures increased with 2 degrees at 371 meters depth. The main research question is: What oceanographic processes can explain the temperature increase in the Western Ross Sea within EC-Earth3?
To explore this, we formed three hypotheses. The first hypothesis is based on atmospheric warming. The second hypothesis is based on warming inflowing waters. The third hypothesis is based on a connection between a Ross Gyre change in EC-Earth3 and the Ross Sea temperatures.
We analyzed relevant variables of an EC-Earth3 climate run with SSP5-8.5, comparing the two different time periods 1970-1990 and 2080-2100.
We found that the increased temperature in the Western Ross Sea in EC-Earth3 is caused by a change in ocean circulation related to the Ross Gyre expansion and presumably Ekman transport. Next to that, the temperature increase is caused by local bathymetry, meltwater presence and the configurations of the model.
This research show the importance of including meltwater perturbations and bathymetry sensitivity in climate models.

Table of Contents

1. Introduction

In the last decades climate change research has become increasingly important. The consequences of climate change have had impact on natural and human systems in the past (Pörtner et al., 2022) and future impacts must be assessed. In order to make predictions about our future it is essential to finetune our understanding of global and local oceanographic systems, as they are important links in our climate system (Bigg et al., 2003). The oceans are a buffer in the global climate system, they are capable of storing heat energy (Bronselaer & Zanna, 2020). The IPCC report, published in 2021, states that the global oceanic heat content (OHC) increased since 1971. Generally this means an increase in ocean temperature (Fox-Kemper et al., 2021). The oceans are even responsible for the uptake of more than 90% of the heat energy accumulated in our climate system between 1971 and 2016 (Riser et al., 2016). This heat content of the oceans translates to (amongst others) global mean sea level rise and globally this is a problem. The cause of this is the thermal expansion of seawater but also the melting of the terrestrial cryosphere (Fox-Kemper et al., 2021). Particularly at the poles there is a relationship between OHC, and thus ocean temperature, and ice loss on land (Meredith et al., 2019). Here, ocean water is in contact with the ice sheet on land through the ice shelves, where the ice shelves serve as buttresses on which the (Antarctic) ice sheets are leaning. There is a continuous outflow of ice from the sheet to the shelves (green arrows in Figure 1), this is induced by gravity, and this is how the shelves gain mass. Snowfall accumulation on top of the ice shelves thickens the ice shelves as well. The ice shelves lose mass mainly through calving (ice shelf break-off), and basal melt of the ice shelves (subsurface melting) (Rignot et al., 2013). The Antarctic ice sheet and ice shelves are in balance when the net mass gain and loss are equal. When ocean temperatures increase, calving and basal melt are increased as well and the balance will be off (Rintoul et al., 2016). The mass ablation will increase: the extent of the shelves decreases and they become thinner. Consequently, they are less of a buttress and the ice sheet becomes unstable as well, resulting in a faster outflow and the net loss of land ice. The Antarctic contribution to sea level rise is still an active field of research.

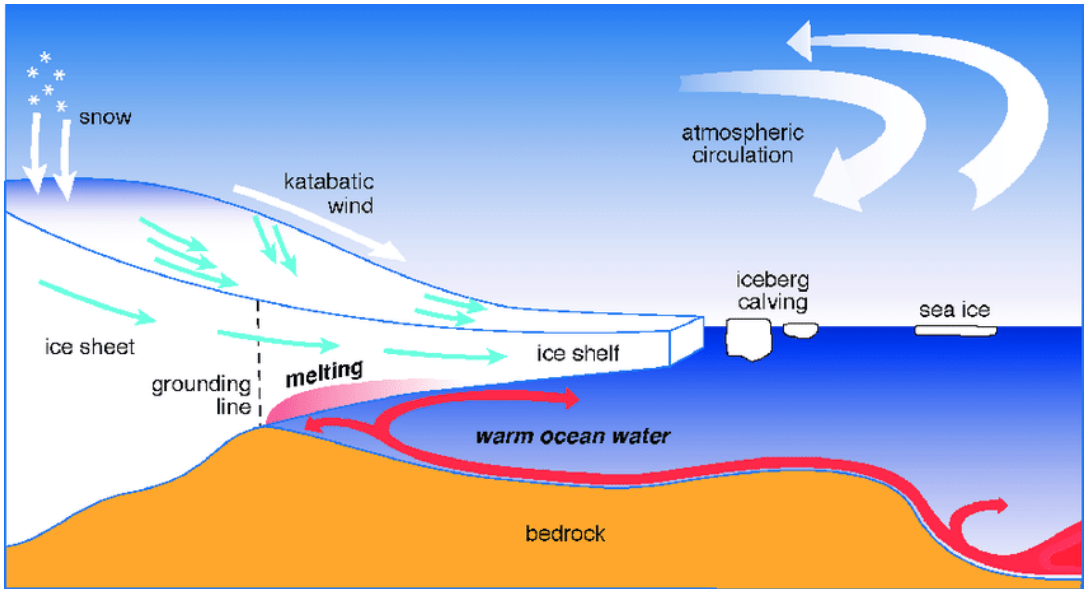

Figure 1.(National Academies of Science Engineering and Medicine, 2015). *Schematic side view of Antarctica. This figure shows the ice flow out from the ice sheet towards the ice shelf and (green arrows) and basal melt underneath the ice shelf (red).*

1.1 Temperature increase in EC-Earth3 and comparison to other CMIP6 models

EC-Earth3 is a global climate model that is part of CMIP6 (sixth Coupled Model Intercomparison Project) (Wyser et al., 2020). CMIP is a framework of experiments that is designed to study and assess coupled climate models with simulation data (O'Neill et al., 2016). There are several climate models part of this framework and they are constantly compared to one another. CMIP6 is the sixth phase of intercomparison project and EC-Earth3 is the third version of the climate model EC-Earth maintained a European consortium.

In an idealized meltwater perturbation experiment around Antarctica with a time span of 150 years in EC-Earth3, the ocean temperatures raised at a depth of 371 meters (Lambert et al., n.d.). In the Ross Sea this temperature rise was considered extreme (2 degrees) compared to the other regions in Antarctica. Especially in the Western Ross Sea and at depth the temperature increases rapidly compared to the surface temperature.
All CMIP6 models show a global warming trend, but in the Ross Sea temperatures are more divers. Figure 2 shows EC-Earth3s' Ross Sea ocean temperatures in blue compared to the ocean temperatures of a subset of CMIP6 models (see sections 2.1, 2.2.2 and 2.2.4 for the configuration of this figure). EC-Earth3 is one of the models that shows higher ocean temperatures, and it shows a rapid increase after the year 2050. All other models show an increase in ocean temperature as well. Some more rapid, like NorESM2-MM, CAS-ESM2-0 and CMCC-ESM2, than others.
Döscher et al., (2022) compared EC-Earth3 to ERA5, and found it has a global mean temperature bias of 0.5 K. ERA5 is a climate reanalysis that is based on a large record of historical observations (Hersbach et al., 2020). The bias is mostly because of a warm bias in the Southern Ocean and Antarctica, however most of the CMIP6 models show a bias in the Southern Ocean (Hyder et al., 2018).
It is necessary to find out what happens to the Western Ross Sea in EC-Earth3 with a more realistic future scenario, as a large temperature increase would have many consequences (section 1.2 and 1.3). Therefore, the main question for this research is: what oceanographical processes within EC-Earth3 are responsible for the Western Ross Sea temperature increase.

1.2 Ross Sea

The Ross Sea is an embayment in Antarctica between 160E and 150W (Figure 3). It lies above the continental shelf (Table 1 [p. 11] and Figure 2), and it is almost all year round entirely covered with sea ice. It is very difficult to obtain data from measurements in this region as the sea ice forms an obstruction. Currently the only way is to place tracing sensors on seals (Charrassin et al., 2008). It is a very remote region, the data available is mostly acquired by satellites or ocean models. The bathymetry shows great variety (Figure 3): the depth goes up to a thousand meters and the highest ridges are four hundred meters deep.

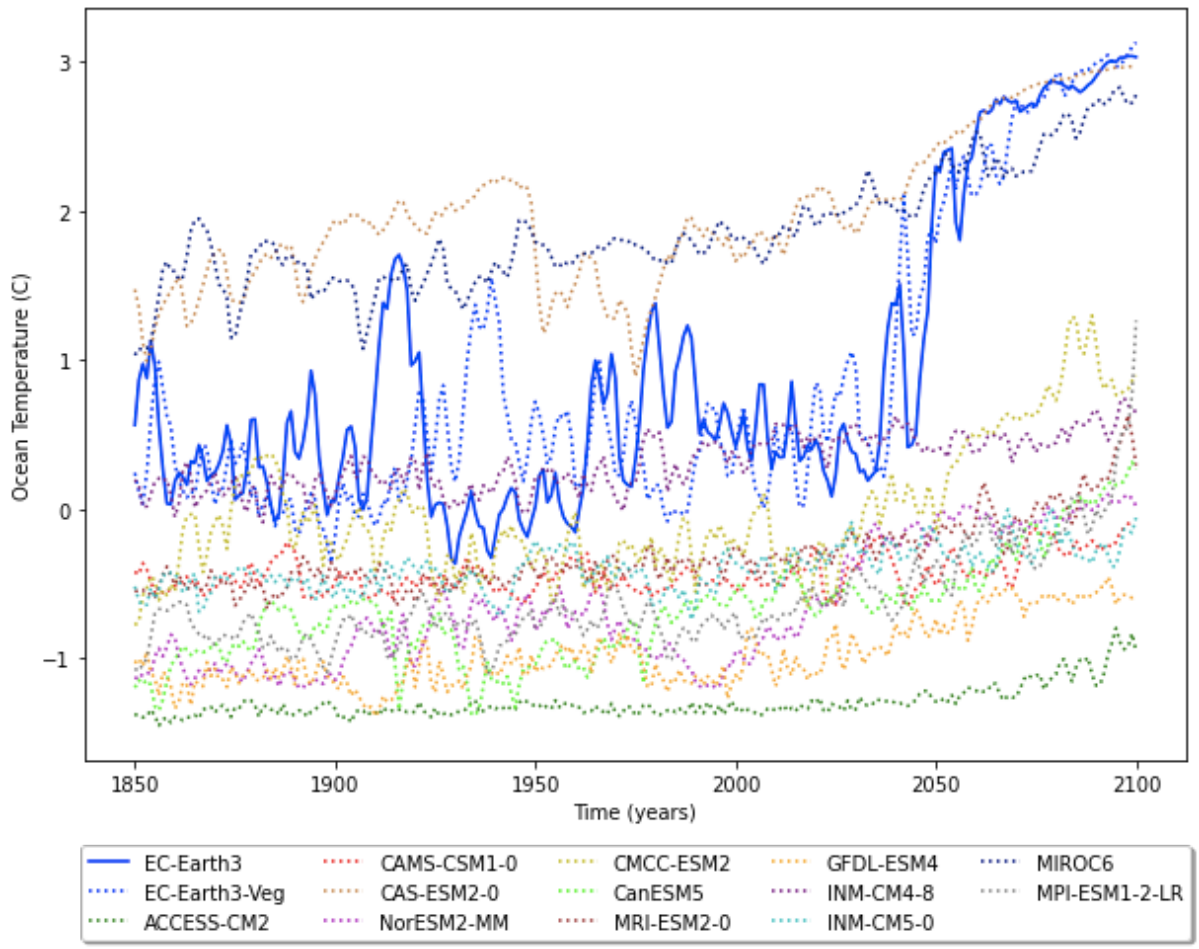

Figure 2. A subset of CMIP6 models ocean temperature for the Ross Sea at a depth of 400-700 meters from the year 1850 to 2100. EC-Earth3 is highlighted in blue and shows the most rapid increase in ocean temperature.

1.2.1 Oceanographical setting

The Ross Sea is situated South of the Ross Gyre (Figure 4) which is one of the two larger gyres of Antarctica that facilitate Southward transport of a relatively warm water mass called the Circumpolar Deep Water (CDW) (Figure 5) (V. Gouretski, 1999). These gyres are sea surface height depressions resulting from atmospheric pressure that on the Southern hemisphere result in cyclonic circulations (Coriolis effect). Changes in the Ross Gyre will probably be felt in the Ross Sea (Dotto et al., 2018). The gyre is a dynamic area that influences the Antarctic Slope Current (ASC). The ASC regulates the flow towards the Antarctic coastline (Thompson et al., 2018), it is closely connected to the cross shore and alongshore transport across the whole of Antarctica. It is a surface current that flows in a anti-clockwise rotation around Antarctica (for the Ross Sea form East to West). All Antarctic ventilation is influenced by the ASC.

The Antarctic Circumpolar Current (ACC) flows in a clockwise rotation around Antarctica and consists of multiple fronts (jet-currents) that are bathymetry steered (Gille et al., 2016). It is the outermost current around Antarctica separating water masses that differ in temperature, salinity and density properties.

The Ross Sea is currently a region where dense deep water is formed: the Antarctic Bottom Water (AABW) (Figure 5) (Orsi & Wiederwohl, 2009). The AABW is part of the global overturning circulation (Talley, 2013) and is thus of importance to the global climate.

1.2.2 Ross Ice Shelf

The Ross Sea is in contact with the Ross Ice Shelf and has a direct impact on it. The Ross Ice Shelf is the largest ice shelf of Antarctica and has a thickness of several hundreds of meters (Rignot et al., 2013). The stability of ice shelves is important for the stability of ice sheet as described in section 1 (Dupont & Alley, 2005).

Basal melt occurs when water with a temperature higher than the local freezing point has access to the bottom of the ice shelf, the cavity. This is located underneath the ice shelf and above the bedrock (Figure 1). In the cavity, ocean driven melting is controlled by thermodynamic processes and circulation, which are mostly unobserved (Stevens et al., 2020). Stevens et al. (2020) shows that currently the Ross Ice Shelf is stable. They measured the ocean temperature in the basal boundary layer (approximately 15 to 20 meters beneath the Ross ice shelf) generally to be close to the local freezing-melting point.

1.2.3 Primary production

Not only can the ocean act as a buffer for temperature, but it is also a buffer for CO2. The Ross Sea has the highest primary productivity in the southern ocean (Ingrosso et al., 2022), and so, is one of the largest Antarctic CO2 sinks. Primary production is highly sensitive to ocean temperature, consequently, any changes in ocean temperature alter the CO2 uptake in the Ross Sea (Kwiatkowski et al., 2020). Kwiatkowski et al., (2020) also demonstrate that most of CMIP6 models (see section 1.2) show increased stratification globally due to enhanced warming. This restrains nutrients and subsurface oxygen ventilation in the upper ocean and will lead to a decrease in CO2 uptake.

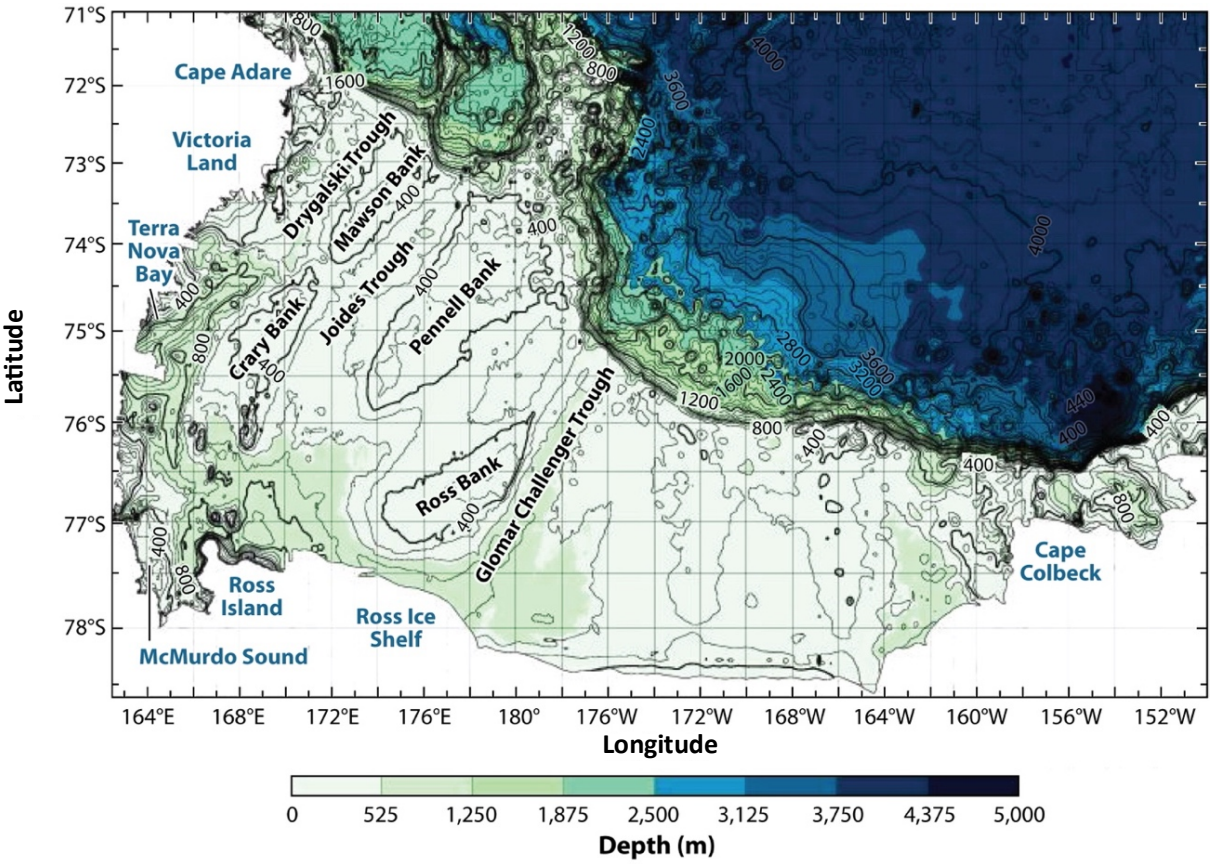

Figure 3. Ross Sea bathymetry map (based on ETOPO1 bathymetry), 100m contour interval. Shelf break visible from Cape Adare to Cape Colbeck along the 1000m depth contour line. Adapted from Smith et al., (2014)

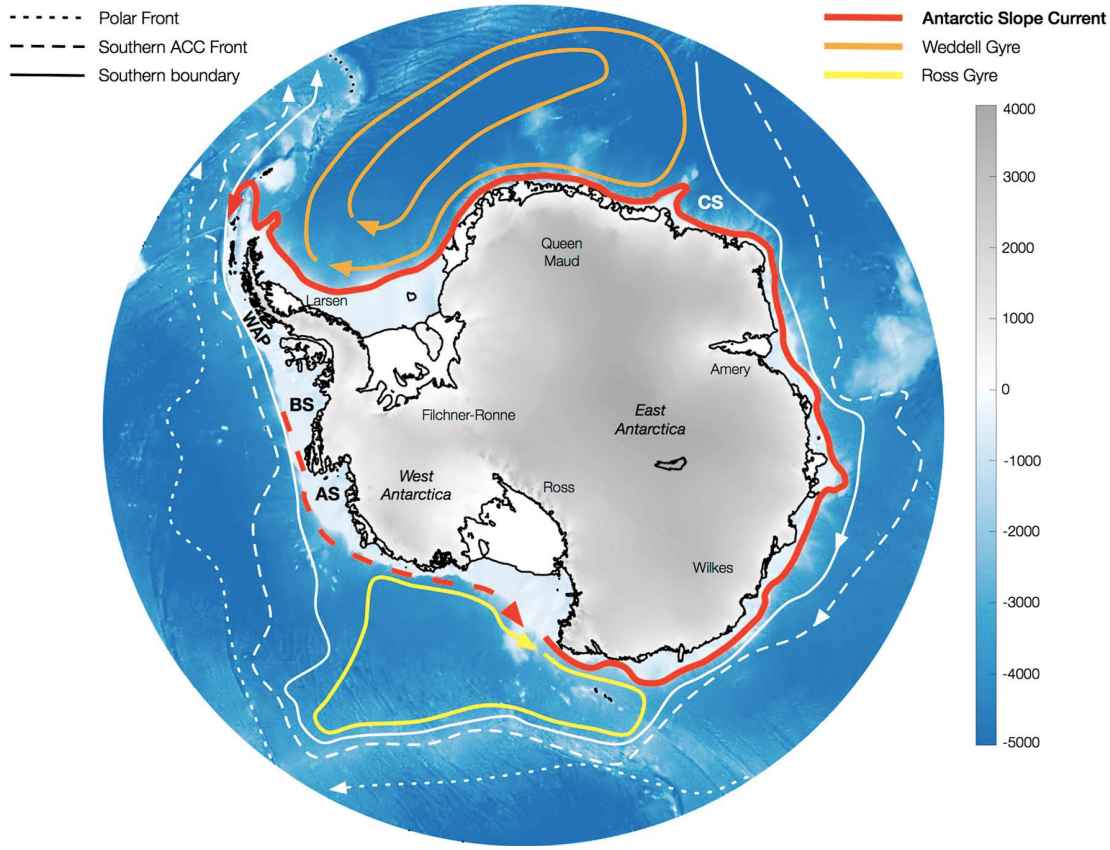

Figure 4. Top view Oceanographical setting Antarctica. The ASC is dashed in front of the Ross Sea because of their uncertainty of the starting point of the ASC at the beginning of their reserach. The continental slope is the transition between light and dark blue in front of the coast. AS is Amundsen Sea.(Thompson et al., 2018)

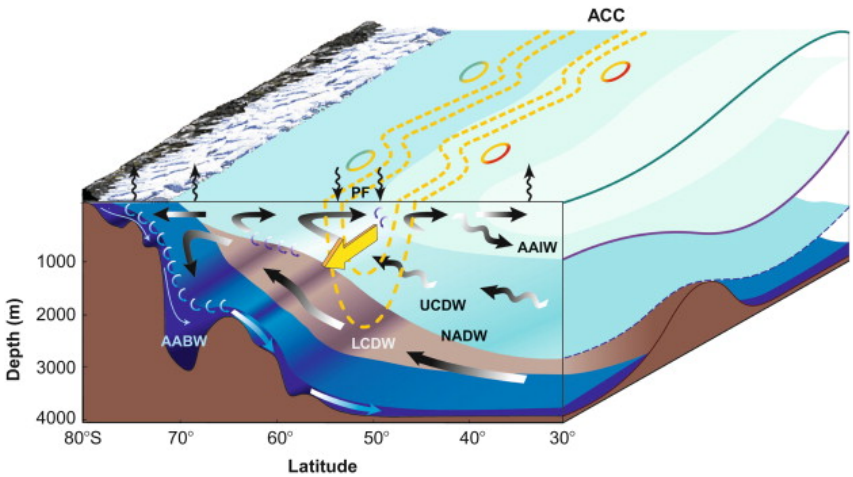

Figure 5. Cross section through Antarctica and adjacent Southern Ocean. Antarctic currents and water masses are presented in this figure. The black arrows indicate the displacement of the water masses, the yellow contours represents the ACC that flows in the direction of the yellow arrow. On the left in white the ice shelf and sea ice are floating on top of the ocean. UCDW and LCDW are Upper and Lower CDW respectively. AAIW is Antarctic Intermediate Water, NADW is North Atlantic Deep Water. (Rintoul et al., 2016)

1.3 Goal and hypotheses

Changes in the Ross Sea could thus have global impact. Changes in the Ross Sea have consequences for (not only Antarctica, but also for) models that use EC-Earth3s' outflow as inflow (for example an ocean-ice sheet dynamics model), coupling earth systems in models still is a challenge.

Our goal is to find out what oceanographical processes gave rise to the temperature rise in the Western Ross Sea in EC-Earth3 in a realistic future scenario. We have formulated three hypotheses that could explain the temperature rise in the Western Ross Sea separately or together.

1.3.1 Atmospheric warming impact on water temperature

It is known that global warming will increase temperatures (almost) everywhere on earth. Li et al. (2021) explains that through Rossby waves teleconnections exist to Antarctica so that climate change elsewhere is also felt in Antarctica. The increase of greenhouse gases (GHG) raises the atmosphere temperature and this in turn increases water temperatures. There is a heat flux between the atmosphere and the ocean, and water is known to be able to store heat (Thorpe, 2005). Increased atmospheric temperatures are already influencing melting rates in Antarctica (Milillo et al., 2022). Sea ice forms a barrier between ocean and atmosphere and so, the exchange of heat would be delayed or not even take place. When there are changes to the sea ice cover (decrease or increase), we expect this would be seen directly in ocean temperatures. Therefore, we want to assess if sea ice concentrations are connected to the temperature increase in the Western Ross Sea in order to detect the influence of the atmosphere on the temperature rise.

1.3.2 Source water increased in temperature

Not only the atmosphere but also ocean temperatures elsewhere increase. All waters in the oceans are impacted by climate change. Through the global ocean circulation and more local circulations explained in section 1.2.1, this might end up in the Ross Sea. In other words: the source water of the Ross Sea, which is the CDW (transported by the ASC), could already have an increased temperature before entering the Ross Sea. This could lead to a general temperature increase in the Ross Sea, and thus maybe add to the Western Ross Sea temperature increase.

1.3.3 Ross Gyre change impact on circulation in Ross Sea

The circulation of the water itself in and around the Ross Sea might also influence ocean temperature. The circulation determines the location of the water masses. Previous research on the Amundsen Sea attributes the UKESM1 (another CMIP6 climate model) temperature increase to the expansion of the Ross Gyre (Felipe et al., 2022). The expansion found is induced by intensified anthropogenic trends in westerly winds (Holland et al., 2019)(Naughten et al., 2022). All three papers suggest that this increases CDW transport onto the shelf and so the ocean temperature of the Amundsen Sea increased. We want to see if something similar might happen in the Ross Sea and therefore, we will analyze whether there are any changes in the Ross Gyre in EC-Earth3. If there is a change, we want to find how this impacts the circulation within the Ross Sea, and if this can explain the increase in temperature.

2 Methods

To analyze the hypotheses, we used EC-Earth3 data to produce figures (top views and cross sections) so that the processes within or close to the Ross Sea would be visible. First, we will explain the EC-Earth3 model and thereafter how we used and processed the output. Beneath, the definition list is presented (Table 1).

Table 1. Definition list

Term	Definition
ACC	Antarctic Circumpolar Current. This current flows in a clockwise rotation around Antarctica.
ASC	Antarctic Slope Current. This current follows the slope of the shelf of Antarctica and flows in an anti-clockwise rotation around Antarctica
Baroclinic condition	Pressure gradient caused by density difference of the water.
Barotropic condition	The difference in sea surface height in the ocean creates a pressure gradient (from high to low)
Barotropic Stream function	A stream function used in a barotropic condition. The barotropic pressure gradient creates a flow. Streamlines can be plotted with this function, along which the value of this stream function is constant. Along these lines the water flows with the same velocity.
CMIP	Coupled Model Intercomparison Project. A project to compare Climate Models around the world, maintained by different institutions, to increase the quality of them.
Continental Shelf	Extension of the Continental Plate where the ocean bed is at approximately <1000m.
Ekman transport	In the case of the ocean, Ekman transport is the net direction in which the water is transported, induced by the combination of Coriolis and a drag force at the surface by wind.
Ice sheet	Land ice covering Antarctica (in this case)
Ice shelf	Floating extension of the ice sheet, into the ocean
Katabatic wind	This wind is cold air that moves due to the pressure gradient force and the gravitational force along a slope. It is commonly found in Antarctica and flows in a land to sea direction.
NEMO	Nucleus for European Modelling of the Ocean. This is a framework of functions to model the ocean in climate studies.
Ross Gyre	An ocean gyre at the Northern edge of the Ross Sea. It rotates clockwise between 170E and 140W (Viktor Gouretski, 1999)
Sea ice	Ice formed at sea, it is frozen sea water.
Sea ice cover	Amount of ocean area covered with sea ice (in percentage)

2.1 EC-Earth3

2.1.1 Workflow EC-Earth3

EC-Earth3 incorporates other models to match reality as well as possible, they are all coupled together. NEMO3.6 and LIM3 represent the ocean and sea-ice components respectively, the other components present in EC-Earth3 are atmosphere and land surface and are represented by IFS 36r4 and HT-ESSEL (Döscher et al., 2022). EC-Earth3 uses input according to the IPCC standards, all CMIP6 models have the same forcing. Forcing datasets are made available in several databases (Appendix 1). For example, the greenhouse gas forcing concentrations are obtained from historical atmospheric concentrations (Meinshausen et al., 2017). The output of EC-Earth3 contains many variables that cover all oceans on the planet. They can be visualized and analyzed separately. See the workflow of EC-Earth3 in Figure 6.

At the moment EC-Earth3 lacks an ice sheet model. This means that meltwater needs to be generated in another way. In EC-Earth3 Antarctica is constructed as a white mountain with an upper limit of snowfall. Once this upper limit is crossed, the excess snowfall becomes runoff and flows directly into the ocean as meltwater.

Next to that, there are no cavities under the ice shelves where most of the interactions between ocean and ice sheet occur. Instead, the border between land or ice sheet and the ocean is a vertical wall. This will be further discussed in the discussion (section 4.9.1).

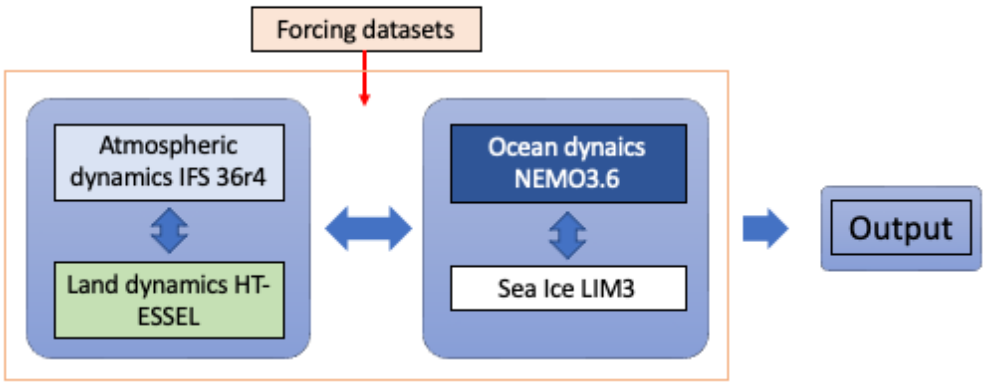

Figure 6. Flowchart of EC-Earth3 (workflow) with model names of incorporated models. EC-Earth3 uses forcing datasets (IPCC) as input, this is processed by the coupled models, and gives output in separate variables covering all the oceans.

2.1.2 Configuration

We analyzed several individual variables with data from the r1i1p1f1 EC-Earth3 climate run. We used the historical run; observations are added to the is the preindustrial control (pi-Control) run.

For the future we used the SSP 5, this is the fifth and highest GHG emitting scenario. EC-Earth uses five different scenarios, according to the Intergovernmental Panel on Climate Change (IPCC) scenarios. These are Shared Socio-economic Pathways (SSPs) and range from low to high socio-economic challenges for adaptation and from low to high socio- economic challenges for mitigation. Moreover, the highest forcing level is used, 8.5 W/m2, so that the scenario is called SSP5-8.5. These worst-case scenario settings are used to identify the processes in the model, as they are probably best expressed in the highest scenario.

The resolution of the r1i1p1f1 EC-Earth3 climate run is 1 degree.

2.2 EC-Earth3 data processing

2.2.1 Ocean cross sections

The latitude and longitude are dependent on both i and j; an example is given in Table 2 with a j value of 7 with different i values. EC-Earth3 uses a tripolar grid to model the earth as a sphere. These different i values are approximately the span of the Ross Sea. The resulting range of latitudes is sufficient to represent a cross section of the Ross Sea that contains the Ross Bank. In the results, all the figures at this cross section (j=7) will have the caption that contains the latitude of -76.6 degrees to average this out. The same applies for the chosen longitude of 177.8 degrees.
Next to this, the model uses 360 degrees for the longitude instead of 180 degrees on the East and West wind direction. It counts from the Eastern degrees onward. This is convenient to analyze this area as it lies on the anti-meridian.
The alongshore cross sections have a point of view to the North and the cross-shore cross sections to the West and the white area represents the continent. The top views of the 400 - 700 meters interval are a weighted depth average and have Antarctica to the South.

Table 2. Latitude and Longitude dependent on i and j grid points

Grid point	Corresponding latitude or longitude
j=7 (i=79)	Latitude = −76.13216400146484
j=7 (i = 137)	Latitude = −76.98344421386719
i=106 (j=0)	Longitude = 177.17576599121094
i=106 (j=30)	Longitude = 178.4935302734375

2.2.2 Area selection Ross Sea

The northern border is at 76 degrees south, this is chosen here because this way the western cavity is captured, without too many disruptions by the other banks to the north (Figure 2). Knowing that there is a warming especially in the West of the Ross Sea, we split up the Ross Sea in an East and West area to see interaction within the Ross Sea. The border between East and West is the Ross Bank, this is a natural border.
For the visualizations in this research the orientations of the wind rose are used (the West is to the left).

2.2.3 Timeframes

The period of interest in the future is as near to the year 2100 as possible. For the comparison between the historical scenario and the future scenario, we selected two time frames; one in the past and one in the future. When averaged over that time frame, the short-term variability is removed (data is monthly). We chose a frame of twenty years, enough to remove large variability and short enough to stay close to the year 2100. So, the period 2080-2100 was chosen for the future and for the past a relatively stable period (for EC-Earth3 Ross Sea ocean temperatures) was chosen; 1970-1990. Next to that, the IPCC mentions this (1971) to be an onset in global OHC change in the upper 700 meters of the ocean (Gulev et al., 2021).

2.2.4 Depth interval

From previous model observations it became clear that the depth of 400-700 meters experiences the greatest change in temperature (Lambert et al., n.d.), so it is evident to

explore that depth interval. An early-stage temperature analysis was made to confirm this. The 400-700 meters depth layer shows the most rapid increase after the year 2050 and has the highest ocean temperature by the year 2100 (Figure 7).

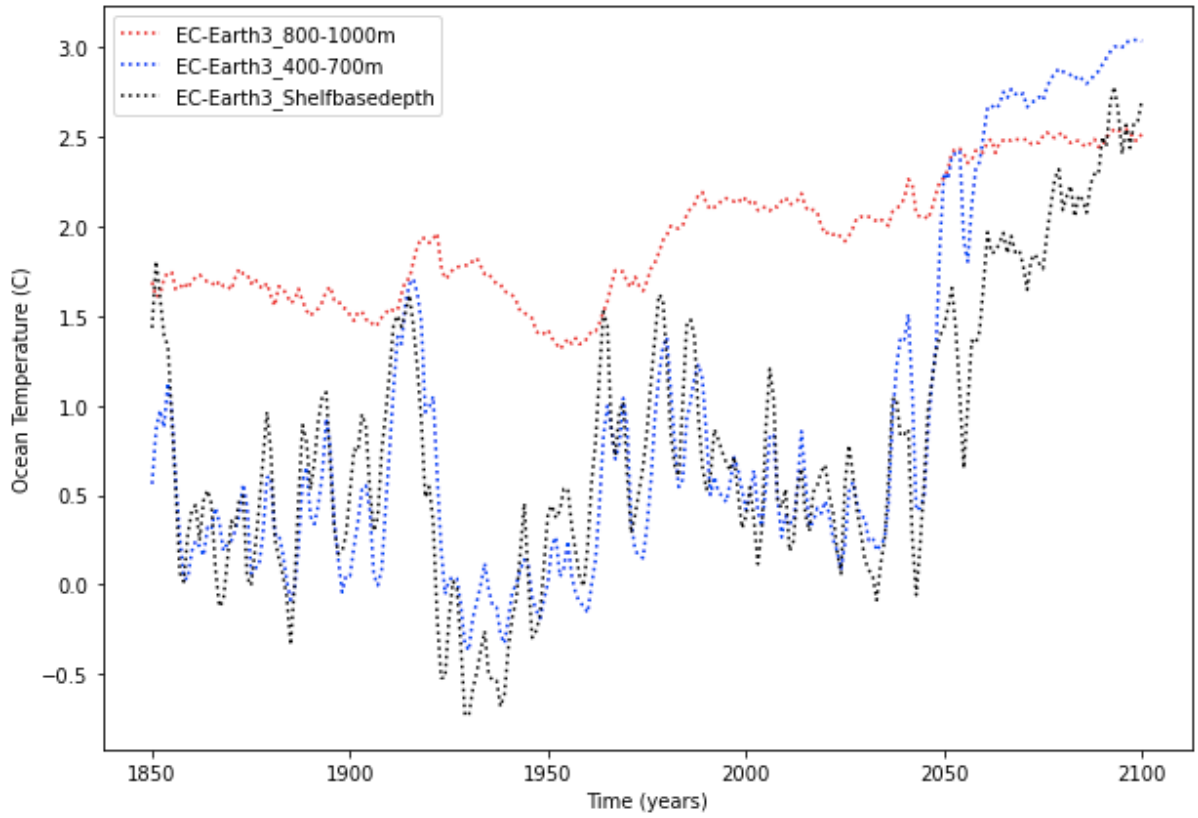

Figure 7. Ocean temperature of Ross Sea for three different depth intervals over time. These ocean temperatures are a weighted average over area and depth. The shelf base depth (shallow) and the intermediate depth ocean temperatures show a different trend than the deep Ross Sea ocean temperature. After the year 2050 all three depth intervals show a different trend.

2.2.5 Variables hypothesis 1

The early-stage (general) temperature analysis is also used for the analyzation of hypothesis 1. We computed an ocean temperature time series from 1850 to 2100 and different cross sections. This is the length in years of the data available. We did this to get insight on where the warm water masses are in the present day and will be in the future. We also made salinity cross sections to distinguish meltwater from 'ocean' water and the two variables together can say something about the stratification. This stratification can show whether there is any influence of the atmosphere on the depth interval. Also, sea ice is an important variable to consider; as it is in between the ocean and the atmosphere, you would expect a correlation between the sea ice presence and the ocean temperature.

After the early-stage temperature analysis we concluded that no further (atmospheric) variables were necessary to analyze.

2.2.6 Variables hypothesis 2

For the second hypothesis we necessary to know the circulation in the Ross Sea itself and to identify the in- and outflow. Velocity plots in several cross sections in the u and v directions were looked at. Also, we plotted the barotropic stream function (Table 1) of the area in front

of the Ross Sea to see the larger scale circulation. To see whether the inflow of the Western Ross Sea is increased in temperature, the temperature of the water mass entering the Western Ross Sea is analyzed.

2.2.7 Variables hypothesis 3

To see if the gyre increased in size or in intensity, the barotropic stream function was used. And since the gyre is a depression there is a height difference, so it is a good variable to identify the gyre. The flow that is created is deflected to the left, due to the Coriolis effect on the Southern Hemisphere. In the plotted figures of this function you can see the gyre and the flow directions. To see the relation with the Ross Sea we also used the velocity plots.

2.2.8 Overview

For clarity Table 3 shows an overview of the variables that have been analyzed for this research per hypothesis.

Table 3. Overview of variables analyzed for this research per hypothesis

Hypothesis	**Variable**
1 & 2	Temperature
1	Salinity
1	Sea ice cover
2 & 3	Velocity
2 & 3	Barotropic stream function

Hypothesis 1	Atmospheric warming
Hypothesis 2	Increased temperature inflowing waters
Hypothesis 3	Gyre expansion connected to Ross Sea circulation and temperature

3 Results

In this chapter we analyze the change from the historical (1970-1990) to the future situation (2080-2100) for the variables discussed in chapter 2. In most cases we chose to show the two time frame situations separately instead of the difference between them in one figure because this way the patterns are visualized more clearly. For every variable we describe the expectations according to the hypotheses and show whether they adhere to them. The green dots in the figures beneath represent the Ross Bank (Figure 3).

3.1 Temperature

For the temperature analysis we show 5 figures (Figure 8 to 12). Figures 8 and 9 show an alongshore cross-section of the temperatures in the historical period and the future, respectively. In the historical situation there is a division between warmer water in the East and cooler water in the West, the Ross Bank seems to form an obstruction. Also, on top of the warmer water in the East there is a layer of cooler water and there is a gradual transition between the two water masses (Figure 8). As the cooler water floats on top of the warmer water this is probably a salinity dominated density stratification. The warmer water is interpreted to be the CDW, as that is usually the warmer water mass present near or on the shelves of Antarctica. The CDW typically has a water temperature of about 1.5 degrees C (Schmidtko et al., 2014). Considering the 0.5K bias (section 1.1) our results show a little higher CDW temperature (2-2.5 degrees C). In the future the transition between these stacked water masses becomes less gradual (Figure 9). The temperature gradient is high; over 150 meters the temperature differs approximately 4 degrees Celsius. In the future, there is a division in water masses only in depth, a stratification in the Western Ross Sea has become apparent. The obstruction has been overcome and the warmer water mass reaches across the Ross Bank. This stratification is already in conflict with hypothesis 1. If the warming was atmospherically induced, we would expect a gradual ocean temperature increase from the bottom towards the surface. Especially with a small warm lid (upper 30 meters) present which is subject to atmospheric warming (Figure 9). If the warming at depth would be the result of the same cause, this ‘warm lid’ would diffusively spread until 400 to 700 meters depth.

Warm water has infiltrated the Western basin, and consequently here the temperature difference between the two time frames is highest (Figure 9): it amounts up to a temperature of more than 3 degrees Celsius. The Eastern part of the Ross Sea increases slightly in temperature, and it does not cool anywhere.

Figures 10 and 11 show the cross section along the longitude 177.8. According to these figures it seems as if the infiltration comes from the North, because it is crossing the Ross Bank from North to South.

Figure 12 is added to show that the entire Western Ross Sea increases in temperature at a depth of 400-700 meters with more than 4 degrees Celsius (locally 5 degrees C). The Eastern Ross Sea does not change so much but still increases in temperature.

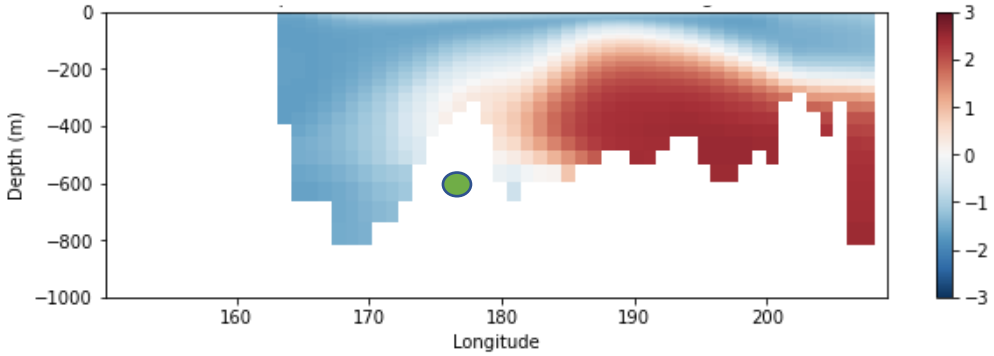

Figure 8. Ocean temperature (degrees C) alongshore cross section, at latitude -76.6, historical. The warmer water mass is interpreted to be the CDW, it is held up by the Ross Bank.

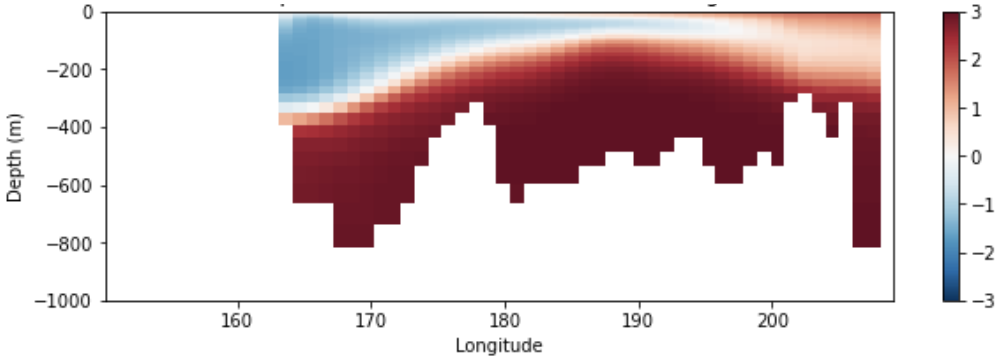

Figure 9. Ocean temperature (degrees C) alongshore cross section, at latitude -76.6, future. The CDW has crossed the Ross Bank and increased in temperature relative to the historical situation.

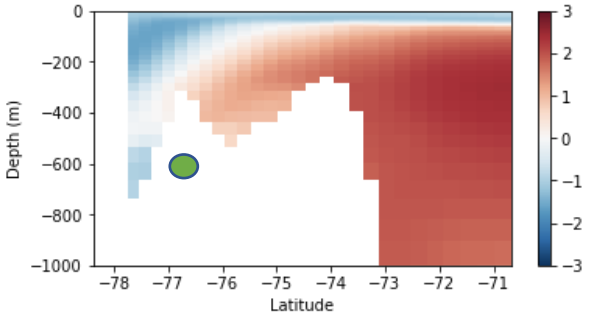

Figure 10. Ocean temperature (degrees C) cross shore cross section, at longitude 177.8 E, historical. The CDW does not cross the Ross Bank

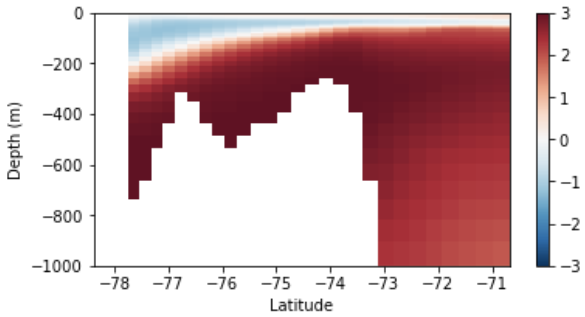

Figure 11. Ocean temperature (degrees C) cross shore cross section, at longitude 177.8 E, future. The CDW crosses the Ross Bank

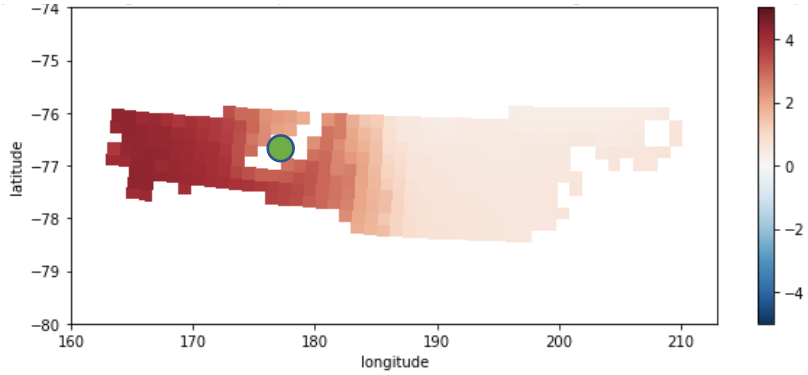

Figure 12. Ocean temperature (degrees C) horizontal cross section, to the North is the Southern Ocean and to the South Antarctica. Top view 400-700 m depth interval (weighted average over depth) of the difference in temperature between historical and future situation. The Western Ross Sea increased in ocean temperature with more than 4 degrees Celsius.

3.2 Salinity

For the salinity analysis, again 5 figures are used (Figures 13 to 17). Figure 13 shows that the West is lower in salinity, which suggests that this water consists predominantly of meltwater. In the future (Figure 14) the Western Ross Sea has become more saline, by approximately 0.4 parts per thousand (ppth) at depth.

Figure 15 shows that the historical Western Ross Sea is well mixed. The salinity is almost at every depth around 34.4 ppth, and this could represent the formation of the AABW, because it is not as low in salinity as meltwater but does have a low temperature. In contrast to the Eastern Ross Sea where there is a slight stratification visible.

The stratification of Figure 9 reappears in Figure 16 so we can now say that on top is the cooler meltwater and below is the wa l' water. Despite our results having slightly less saline values than typical for the CDW (34.75 ppth compared to 34.9 ppth)(Schmidtko et al., 2014), this is still interpreted to be the CDW as this is usually the most warm and saline water present around the Antarctic slope. There is a meltwater intrusion impeding the warming from the atmosphere to continue at depth. Again, this is in conflict with hypothesis 1. Also, the Eastern part of the Ross Sea becomes more stratified. The salinity in the top layer decreases and the layer beneath increases in salinity (Figure 17). This suggests that the meltwater inflow has increased over the years.

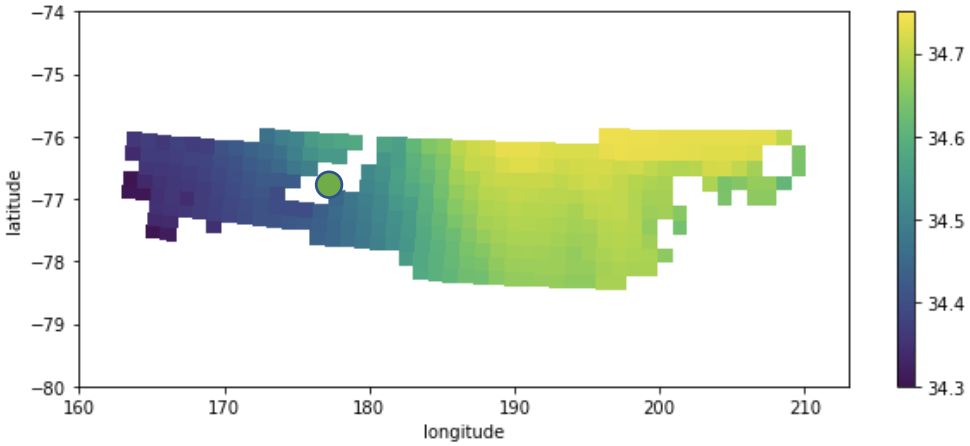

Figure 13. Salinity in ppth in a horizontal cross section. Top view of the 400-700 m depth interval (weighted average over depth), historical. To the left (Western Ross Sea) the low salinity is interpreted to be meltwater and to the right (Eastern Ross Sea) the higher salinity to be the CDW.

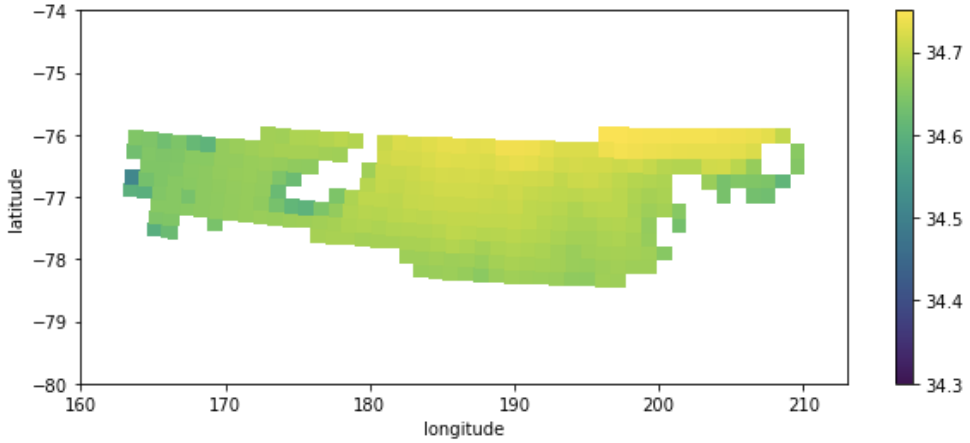

Figure 14. Salinity in ppth in a horizontal cross section. Top view of the 400-700 m depth interval (weighted average over depth), future. The Western Ross Sea increased in salinity relative to the historical situation.

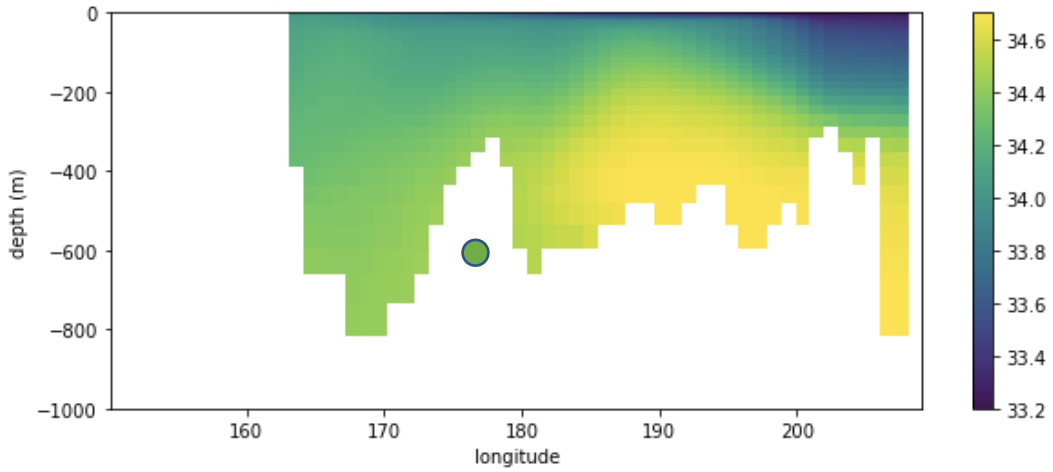

Figure 15. Salinity in ppth in an alongshore cross section. Northward point of view, historical. The Western Ross Sea is well mixed over depth, the Eastern Ross Sea is a little more stratified. The higher salinity in the Eastern Ross Sea is interpreted to be the CDW.

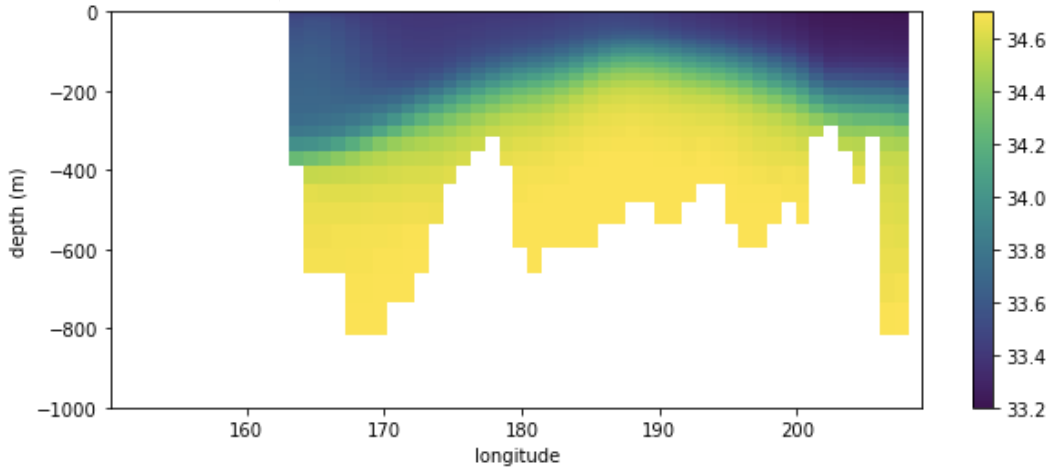

Figure 16. Salinity in ppth in an alongshore cross section at latitude -76.6. Northward point of view, future. The CDW has crossed the Ross Bank and the Western Ross Sea has become stratified.

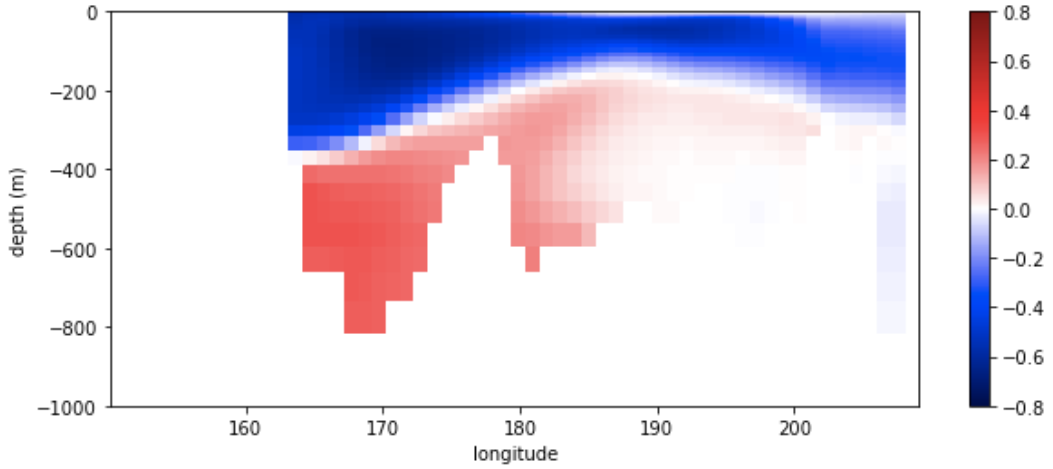

Figure 17. Salinity in ppth in an alongshore cross section. Northward point of view, difference in salinity in ppth between historical and future. The largest differences in salinity can be found in the Western Ross Sea.

3.3 Sea ice cover

As we show in the Figures 18 and 19, the sea ice cover in the Ross Sea changes drastically over the years. There is a large difference between the East and the West, in the West the percentage drops only 10 to 20%, whereas in the East the percentage drops with 60%. We expected the opposite according to hypothesis 1. Less sea ice cover would mean more atmospheric warming influence and thus a warmer ocean.

To this end we also plotted the sea ice cover and temperature over time together (Figure 20). We singled out only the Western Ross Sea to see the local correlation. This does show the decrease of the sea ice cover, but the temperature curve does not match. Sea ice cover slowly decreases while the rapidity of the temperature increase, after 2050, suggests a tipping point. It is important to point out the absolute percentages as well to see whether with this change there is still sea ice cover left or not at all. One can see in Figure 19 that sea ice cover in the Ross Sea from East to West increases from 0% to approximately 55%. The effect of the absence of sea ice cover is shown in 3.4.3 and discussed in section 4.4.

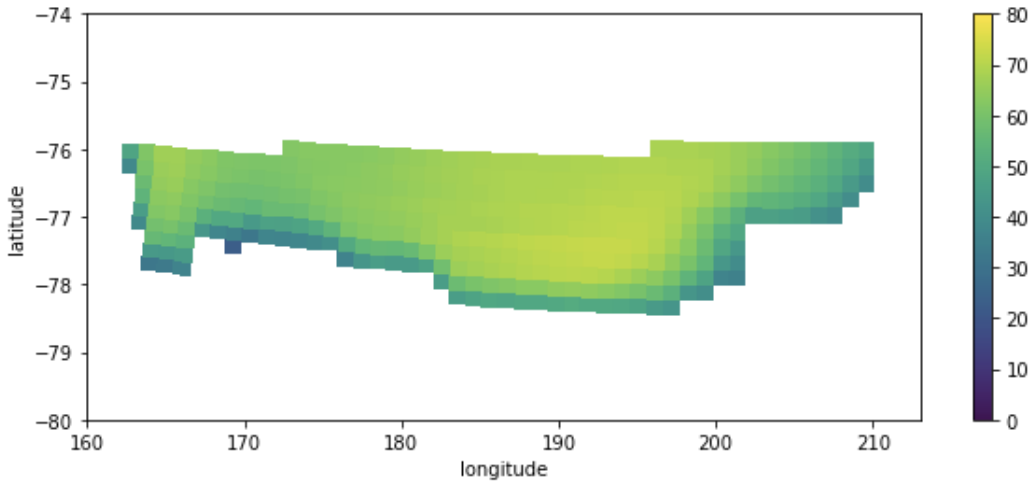

Figure 18. Sea ice cover in percentage in a top view of the Ross Sea, historical. The entire Ross Sea is covered in sea ice averaged over this time interval and almost everywhere the concentration is above 50%.

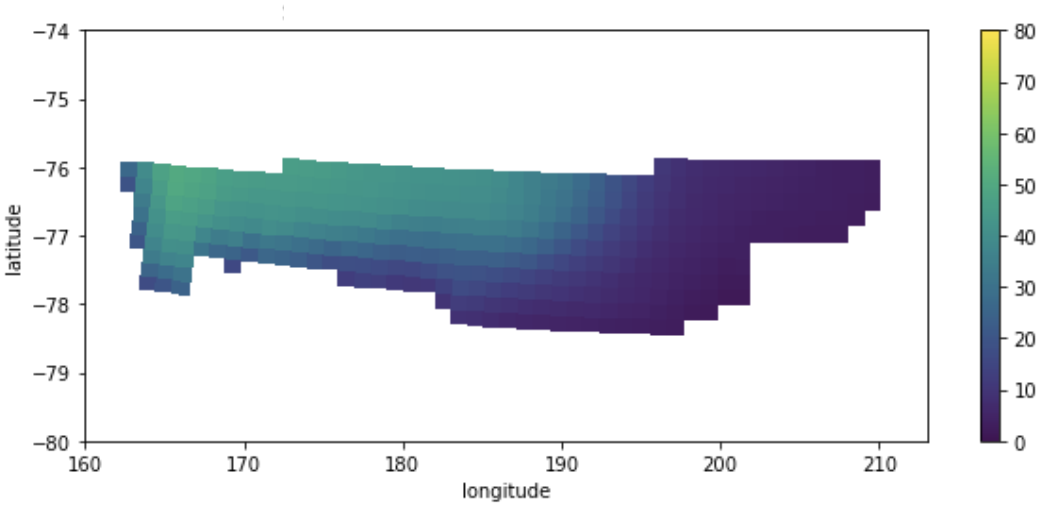

Figure 19. Sea ice cover in percentage in a top view of the Ross Sea, future. In the Eastern Ross Sea almost no sea ice is left and the Western Ross Sea has a cover concentration of no more than 50%.

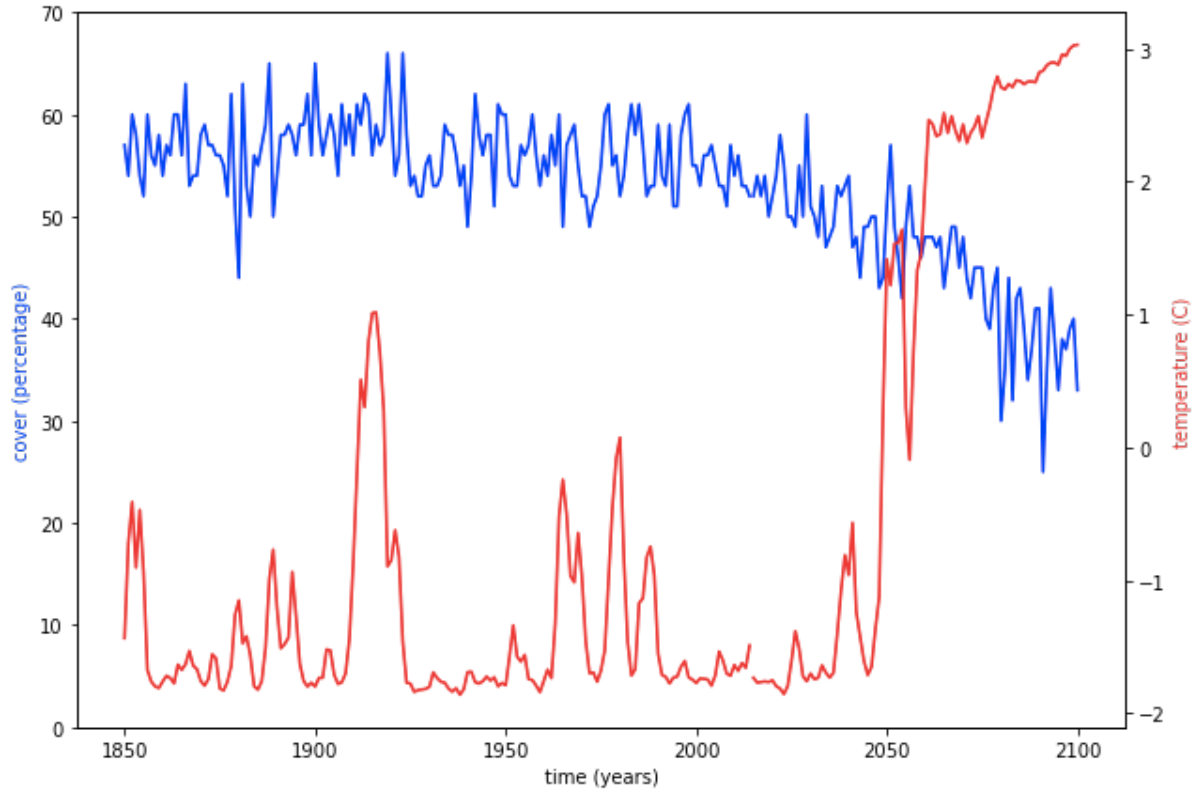

Figure 20. Western Ross Sea ocean temperature and sea ice cover concentration over time. The ocean temperature shows a steep increase after 2050 and the sea ice concentration slowly decreases.

3.4 Flow velocities

We used two types of cross sections to analyze the flow velocities to deduce the circulation and the inflow of the Ross Sea for hypothesis 2. One is in the *x* direction and one is in the *y* direction, both contain plots for the historical and the future situation. The flow velocities are represented by negative and positive values and their associated colors (Table 4). To enhance the visibility of the processes we decreased the maximal velocity on the axis.
This variable has been considered to be able to detect the circulation within the Ross Sea (according to hypothesis 2). The achieved in- and outflow of the Ross Sea will be shown in this section.

Table 4. Flow velocity orientations in EC-Earth3

Orientation	Positive (Green)	Negative (Purple)
X (u)	Eastward	Westward
Y (v)	Northward	Southward

3.4.1 Inflow and outflow

For the inflow of the Western Ross Sea we looked at the *u* and *v* velocities in the alongshore cross section for both the historical and the future situation. These are shown by figures 21 to 24. To the South and West the Western Ross Sea is closed in. To analyze the Northern inflow we looked at *v* and to analyze the Eastern inflow we looked at *u.* Figures 21 and 22 show that the Eastern inflow has strongly increased over time and figures 23 and 24 show the Northern

inflow has (almost entirely) disappeared over time. The latter contradicts the temperature analysis findings about the inflow of the Western Ross Sea, where it seemed the warmer water mass came from the North (Figures 10 and 11). In fact, we show that it originates from the East, crossing the Ross Bank, which matches figures 8 and 9.
The outflow can be deduced from the same figures (Figures 21 to 24). Figures 21 and 22 show the Eastern outflow disappears over time, and figures 23 and 24 show the Northern outflow increases over time.

3.4.2 ASC

The flows visible in these figures (Figures 21 to 24) are interpreted to be the ASC. Our results have a smaller flow velocity magnitude than the ASC has above the slope (10 to 30 cm/s)(Thompson et al., 2018). However, Thompson et al., (2018) state that there is enough evidence (modeling and observational) for the ASC to consist of multiple smaller jets spread over the shelf. We might be looking at such a jet stream. Moreover, it follows other characteristics of the ASC (section 1.2.1). In all four figures we see a strong inflow in the Ross Sea in the East. In the Western Ross Sea we see an additional meander meaning some water enters here, this is interpreted to be a small ASC jet stream that represents the interaction between the AABW and meltwater (Figure 23). The scales for figures 23 and 24 are lowered compared to figures 21 and 22 to show the cores of the currents better.
One can see the pathway of the ASC changing over time. The most important change being the outflow of the ASC of the Ross Sea changing location from (mainly) East of the Ross Bank to (mainly) West of the Ross Bank, or at least it bifurcates. This means the ASC now flows through the Western Ross Sea. The displacement of the ASC ensures an increased transport into the Western Ross Sea, bringing along the CDW. In the historical situation there was an inter-basin difference in ocean ventilation and in the future the basins (East and West) are connected. Apart from that, the strength of the ASC changes, it significantly increases. Logically above a ridge the flow velocity is higher, because of the smaller cross-sectional area, this can be seen in both the historical as the future situations.

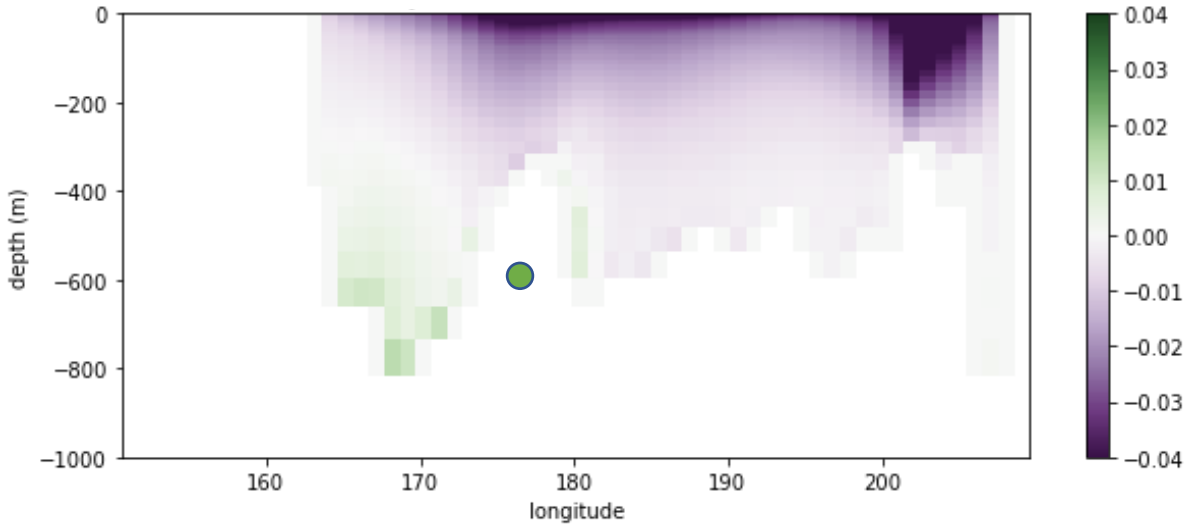

Figure 21. Flow velocity (u) in m/s an alongshore cross section at latitude -76.6. Northward point of view, historical. This figure shows indications for Ekman transport and the ASC.

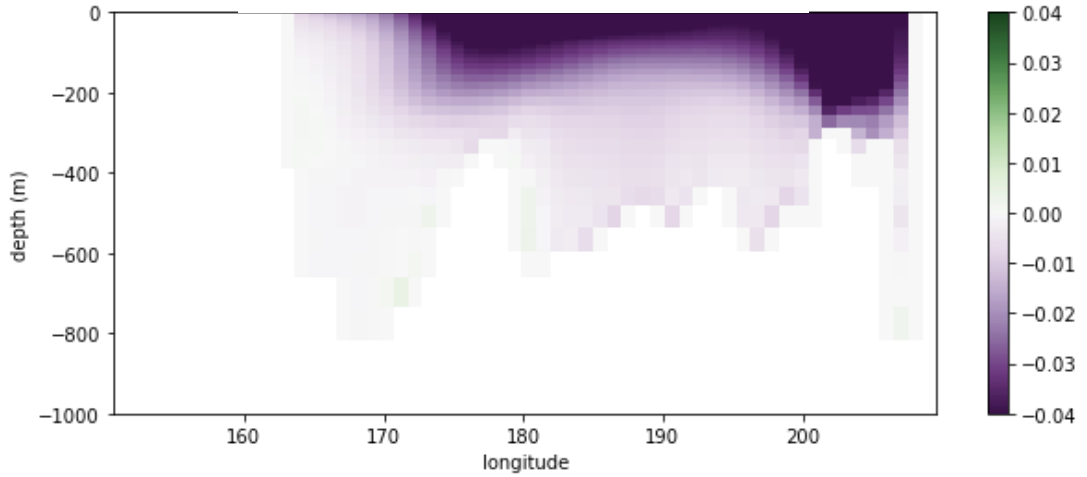

Figure 22. Flow velocity (u) in m/s an alongshore cross section at latitude -76.6. Northward point of view, future. This figure shows indications for Ekman transport and the ASC. The Eastward currents have disappeared and the Westward current has become stronger.

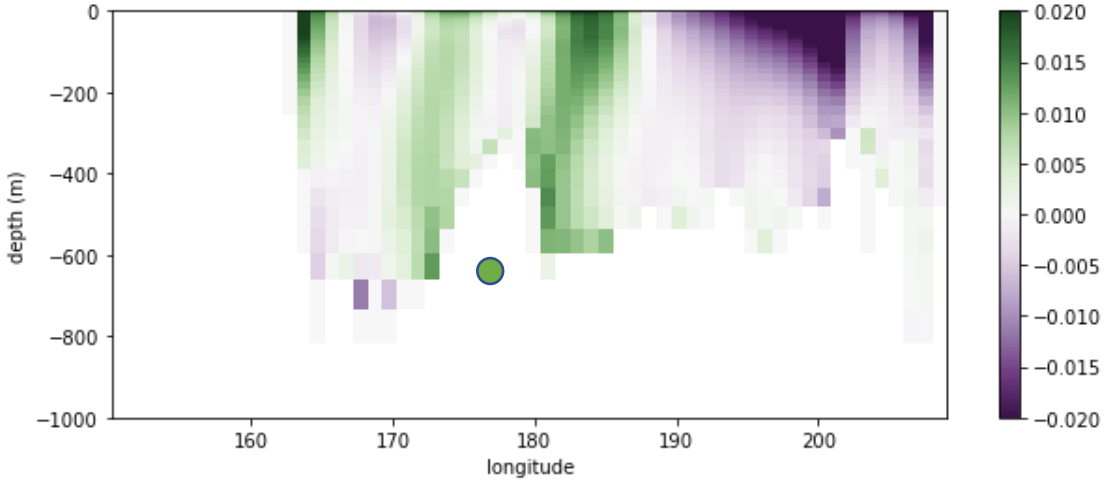

Figure 23. Flow velocity (v) in m/s an alongshore cross section at latitude -76.6, historical. The core currents in the Eastern Ross Sea are interpreted to be (jet streams of) the ASC

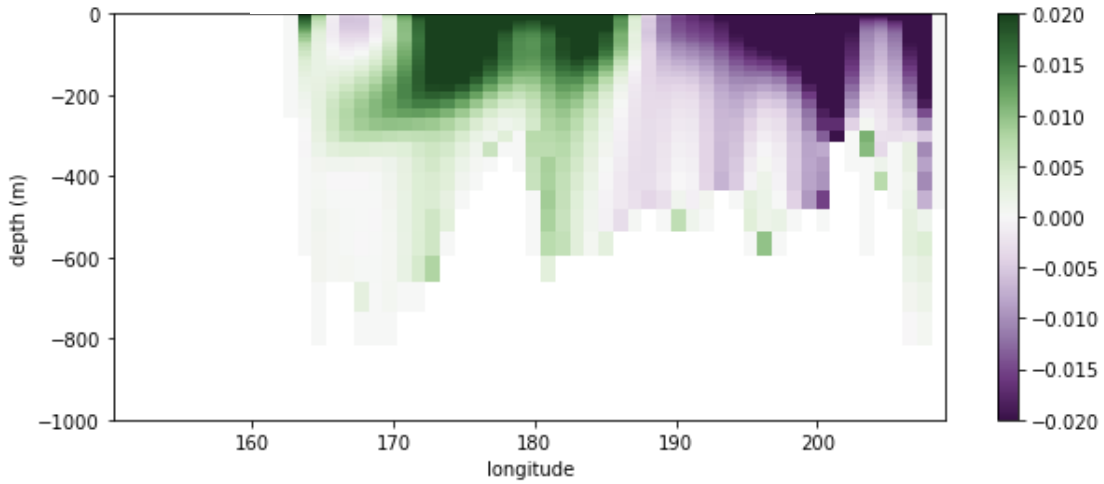

Figure 24. Flow velocity (v) in m/s an alongshore cross section at latitude -76.6, future. The (jet streams of) ASC increased in intensity compared to the historical situation and displaced within the Ross Sea, now exiting the Ross Sea through Western Ross Sea.

3.4.3 Surface stress

Next to the identification of the ASC, we have reason to think we saw Ekman transport. Figures 21 to 24 show a clear intensification of the currents' velocities towards the surface, which is typical for Ekman transport (Table 1). The ASC is thus probably not solely responsible for the increased transport into the Western Ross Sea. We looked at the surface stress variable of EC-Earth3 induced by the overlying atmosphere, sea ice and ice shelf. On the Southern Hemisphere the effect of wind on the underlying ocean is a flow that is deflected to the left, compared to surface stress direction. So for this flow in our results to be Ekman transport, the wind in the *v* direction must have increased positively. Figure 25 shows that this is indeed the case. It would have to be calculated for verification, but this and the strong intensification of the currents towards the surface are strong indications for Ekman transport. In this figure we also plotted the sea ice cover percentage of 15% in the future situation (see also Figure 19) (15% is often used as an indication for the presence of sea ice). The area where sea ice has disappeared matches the area of the most increased surface stress. This shows that the disappearance of sea ice cover enhances wind to have free rein and the surface stress to increase.

The v component of surface stress is dominating, it is an order of magnitude larger compared to the u component (Table 5). The most common Antarctic wind in this direction (v) is the Katabatic wind. This wind could represent the Katabatic wind or an outflow of it, also because there is a height difference between the Ice Shelf and the sea surface (Table 1). Next to that, Farooq et al., (2023) found, with Antarctic Mesoscale Prediction System (AMPS) wind data, the Katabatic wind to be present in the Western Ross Sea.

Table 5. Value ranges of the surface stress in the time frame 2080-2100 for the v and u components.

Component	Value range 2080-2100
V	-0.04 – 0.03 Nm-2
U	-0.05 – 0.15 Nm-2

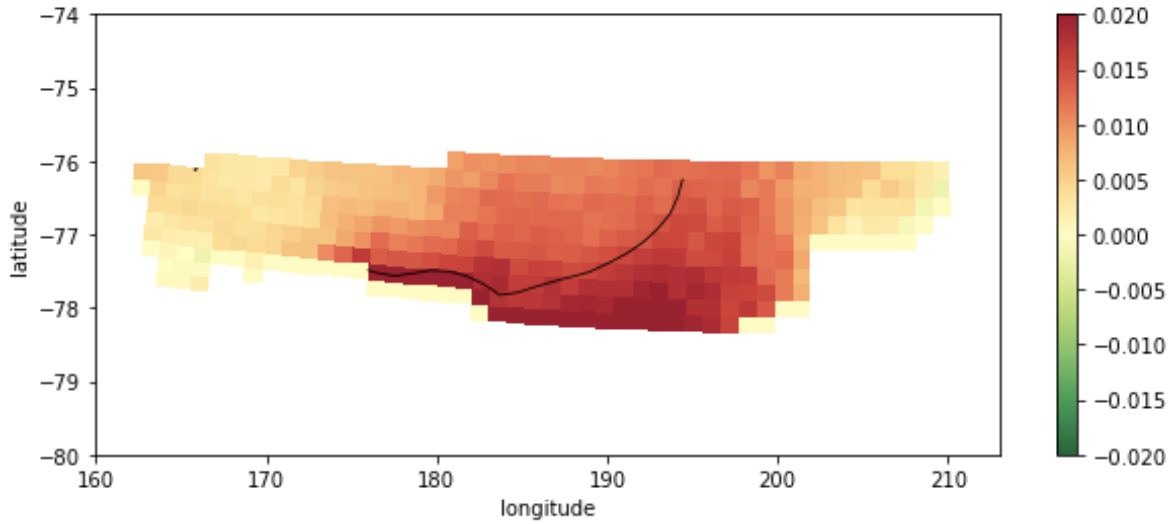

Figure 25. Ross Sea difference in surface stress (N m-2) in v direction on liquid ocean from overlying atmosphere, ice shelf and sea ice. Black line is the sea ice cover concentration mark of 15% of the 2080-2100 time interval. To the right of this line sea ice cover concentration is less than 15%, this matches with the area of the greatest surface stress increase.

3.5 Barotropic stream function

According to hypothesis 3 the Ross Gyre in front of the Ross Sea must increase in EC-Earth3 and this must be felt in the Ross Sea. Again, the historical situation (Figure 26) is put next to the future situation (Figure 27). For a better overview the figures show a larger area than the previous results (white island in top left corners is New Zealand): they fully include the Ross Gyre. Negative values represent a clockwise rotation and positive values represent an anti-clockwise rotation (Table 6). Along each contour line the flow velocities are the same (Table 1).

The figures clearly show an expansion but foremost an intensification of the Ross Gyre. The area containing the darkest orange color has a larger areal spread, the Gyre expands towards the Ross Sea and the shore. The minimum value decreased 1.4e10 kg s-1, 14 Sverdrup, the gradient between the positive and negative values increases. The barotropic stream function values in the Ross Sea are low compared to the Ross Gyre, however the Ross Sea does experience the outer edges of the Ross Gyre. Figure 27 shows a slightly darker orange color for the Ross Sea than Figure 26, this is in accordance with hypothesis 3. Figures 29 and 30 are zoomed in on the Ross Sea and they show this increased influence of the Gyre in the (Western) Ross Sea as well.

Table 6. Rotation of barotropic stream function values

Barotropic stream function values	Positive (Purple)	Negative (Orange)
Rotation	Anti-clockwise	Clockwise

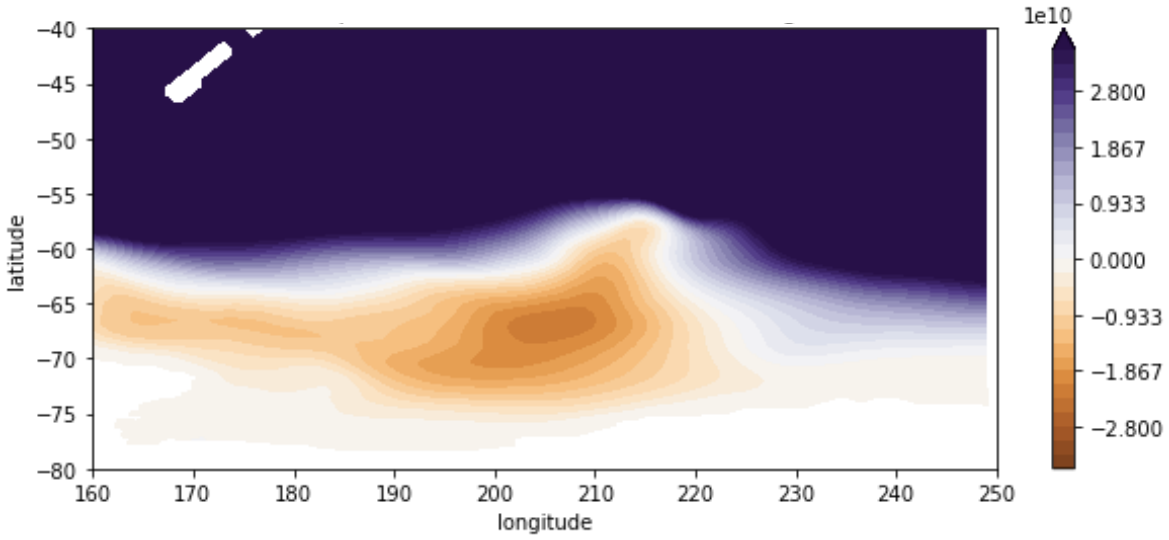

Figure 26. Barotropic stream function in kg/s, historical. This top view covers a larger area, the white area in the top left corner is New Zealand. Orange circulation represents the Ross Gyre. Along each contour line the water flow with the same speed.

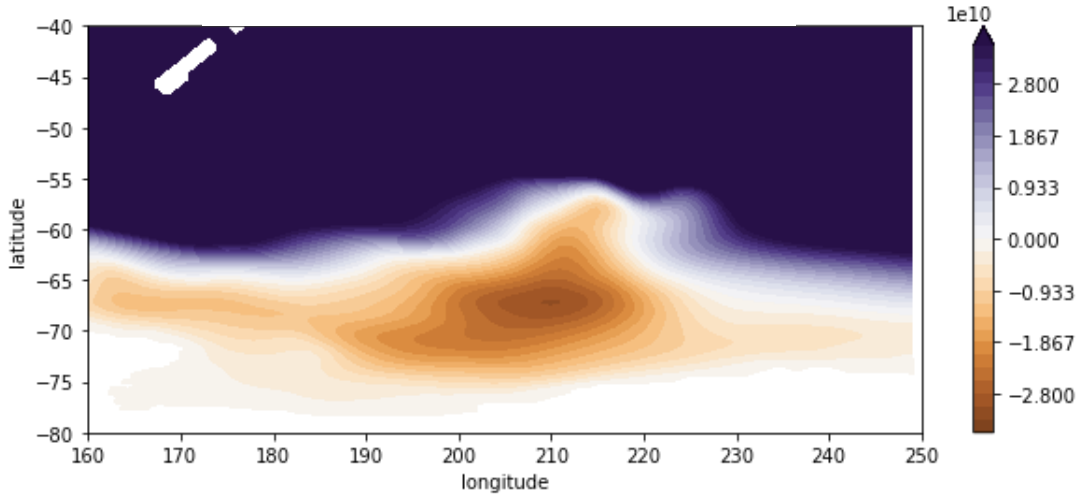

Figure 27. Barotropic stream function in kg/s, future. This top view covers a larger area, the white area in the top left corner is New Zealand. The Ross Gyre increased in size and intensity relative to the historical situation. An expansion towards the Ross Sea is visible.

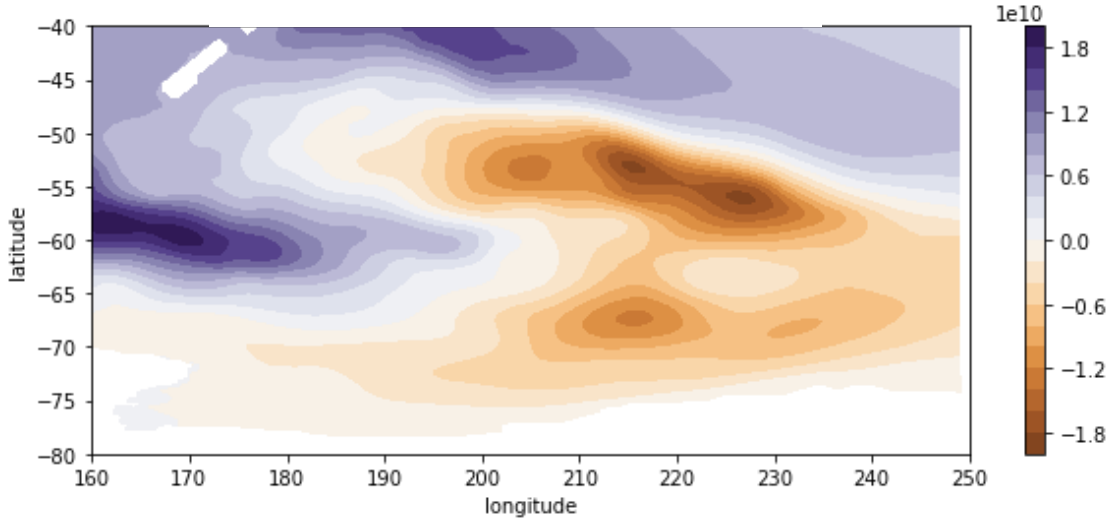

Figure 28. Barotropic stream function in kg/s, difference between historical and future situation. The Ross Gyre increased in intensity and the larger effect in the Ross Sea is visible. North to the Ross Gyre the water flows in a less strong anti-clockwise rotation.

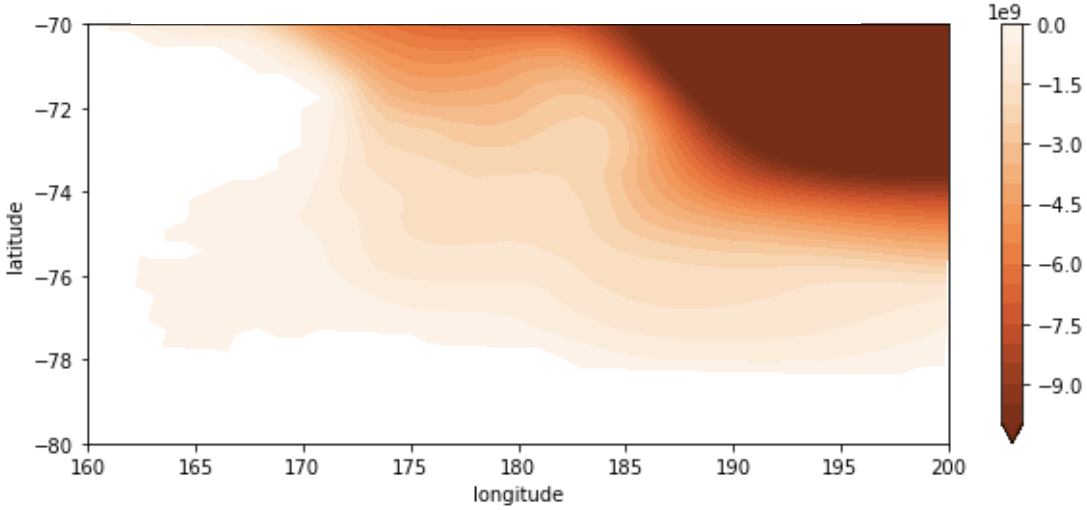

Figure 29. Barotropic stream function Ross Sea in kg/s, historical. Scale is set to show the impact on the Ross Sea

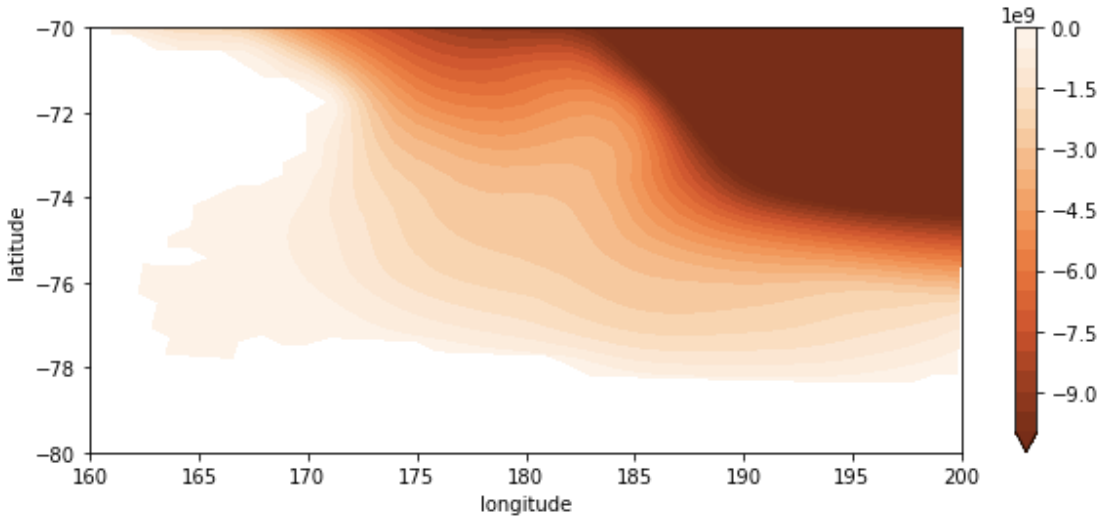

Figure 30. Barotropic stream function Ross Sea in kg/s, future. The impact in the Ross Sea increases, contour lines with a more negative circulation come closer to the coast.

4 Discussion

The discussion chapter is built up in three parts. First, we discuss the hypotheses by merging the results analysis, then explanations for processes identified are given supported by literature. Finally, we will discuss the uncertainties of this research and the possible or needed future research.

4.1 Stratification impedes downward warming from surface

As the general temperature analysis figures show (section 3.1), there is a horizontal stratification in the Ross Sea in the future situation, which contains a warmer and a cooler layer. The salinity stratification is stronger than the temperature stratification. Section 3.2 shows that the upper (cooler) layer is meltwater.

The cold-water layer beneath the surface impedes this diffusive distribution. Thus, one cannot say the rise in temperature of the Ross Sea is connected to direct atmospheric warming and the disappearance of sea ice. The increase in temperature is not continuous over depth nor does it follow a diffusive distribution. The interruption of cold water, the density stratification, means that the temperature increase cannot be caused by sea ice disappearance.

Therefore, there is also no connection to the sea ice cover in the Western Ross Sea. The fact that there is still sea ice present is probably due to the cool meltwater, sea ice becomes an indicator for meltwater presence.

4.2 Temperature increase inflowing waters

The warmer water mass is thus at depth, not the surface, and must have an 'oceanic' and not atmospheric causality. It seems that the Western part of the Ross Sea fills with warmer water over time. The barotropic stream function plots show the waters (in and) around the Ross Sea flowing in an East to West direction. The velocity plots show the inflowing waters to the Western Ross Sea have changed.

However, the inflowing waters of the historical situation have not increased in temperature. We have found that over time the inflowing waters come from another direction, bringing along CDW.

The CDW itself did increase in temperature over time in EC-Earth3. Therefore, we can say that this contributes to the temperature rise as well. However, only with approximately one degree (maximal two degrees) (Figures 8 and 9), this does not match the temperature difference in the Western Ross Sea of more than four degrees (Figure 12). This is because in the historical situation the CDW was not present in the Western Ross Sea. To explain this change the third hypothesis appears to be necessary.

4.3 Ross Gyre increase in size and intensity

Section 3.4.2 states that the ASC changes its pathway and becomes stronger. Section 3.5 states that this is connected to the Ross Gyre expansion, because of the pressure gradient moving South- westward (towards the Ross Sea). Since the Ross Gyre expanded towards the shore and the velocities close to shore (overlapping the ASC flow) became higher, it is very likely that this influences the ASC. The higher velocities of the ASC can thus be traced back to the expansion of the Ross Gyre. This is what is needed for the CDW to enter the Western Ross Sea. From the higher velocities we deduced that the volume of water through the (Western) Ross Sea increased. This results in an increase in temperature because simply said, more (saline) warm ocean water is advected to the (Western) Ross Sea. Resulting in the temperature

increase that is equal to the difference in temperature of the two water masses (meltwater and future CDW).

4.4 Increased transport to the West

An indirect sea ice cover interaction can be found in the Eastern Ross Sea basin. The sea ice disappears even more here than in the Western basin and Figure 19 shows that in most of the Eastern basin no more sea ice is formed. The sea ice formation and melt is due to both atmospheric-sea ice and ocean-sea ice dynamics; increased atmospheric heat enhances sea ice melt (Eayrs et al., 2021). The sea ice displacement in the Ross Sea in our results is probably mostly due to wind influence. Farooq et al., (2023) found that sea ice motion in the Western Ross Sea is predominantly dependent on wind-driven sea ice dynamics.
The absence of this shield means that interaction between atmosphere and ocean can take place. Wind influence (expressed in surface stress) is strongly increased in the future. Wind induces Ekman transport (Table 1), and as mentioned in 3.4.3 there are strong indications for this. This would result in a Westward current on the Southern Hemisphere.
The Ross Gyre intensification and the decreased sea ice cover are thus probably together responsible for the increased transport of warm water into the Western Ross Sea.

4.5 Local OHC

We found another mechanism that might be responsible for the shown OHC (expressed in high temperatures) of the Ross Sea. Normally, CDW that approaches the Antarctic coast cools down (Toggweiler & Key, 2001). This is not the case in the Western Ross Sea in EC-Earth3.
Lecomte et al., (2017) found that sea ice, in combination with fresh melt water, can increase the temperature of the underlying ocean. The sea ice and fresh water form a lid on top of the ocean water, which creates a density stratification. This upper lid impedes the lower water layer to emit its heat to the atmosphere. This means that the ocean temperature would not cool down in the presence of sea ice. Figure 20 shows that this link is weak for the future Ross Sea. As there is still some sea ice left, probably sustained by meltwater perturbations (Lecomte et al., 2017), but overall, it decreases. That which is present in abundance our results is meltwater and probably this functions as a top layer boundary.
The meltwater layer covers a larger depth range in the West than in the East of the Ross Sea (Figures 9 and 16), that is why we arced this area in Figure 31. We do not see that a larger depth range has a larger effect than a smaller depth range.
This process, suggested by Lecomte et al., (2017) could thus apply but then only with meltwater (instead of both sea ice and meltwater) being responsible for the OHC not decreasing.
Another aspect that causes the OHC not to decrease is the fact that the heat cannot be lost by melting the ice shelf either in EC-Earth3 (section 4.9.1).

We created this schematic overview to summarize and illustrate processes responsible for the temperature increase in the Western Ross Sea (Figure 31). This includes the changes in the ASCs' pathway and the meltwater presence forming a lid.

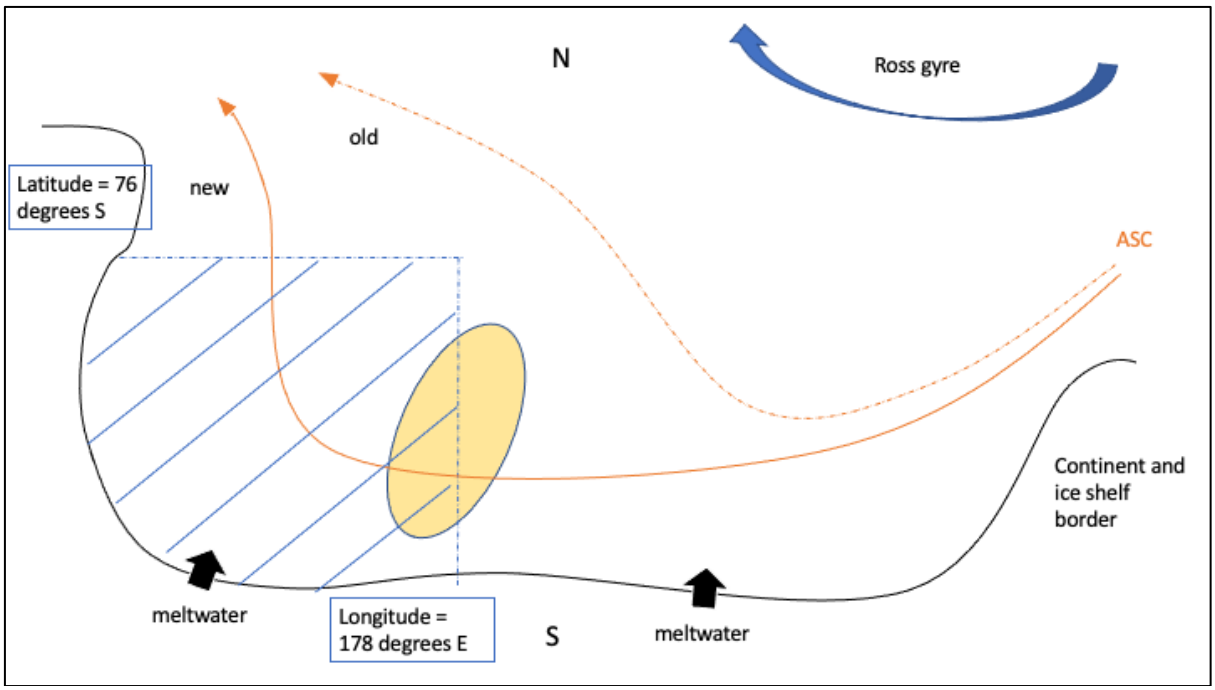

Figure 31. Schematic overview of the Ross Sea containing the changing ASC and the meltwater layer in the Western Ross Sea (left). The yellow oval represents the Ross Bank.

4.5.1 Unmixable water layers

The upper and the lower water layer do not mix because they have different properties. Brine rejection in the little remaining sea ice (seen in Figures 18 and 24) apparently does not redress the salt concentration in the upper layer so that the properties become more resemblant, and the two layers would mix better. Brine rejection is the process of the exclusion of NaCl particles from the ice. Salts are almost insoluble in ice, that is why these particles are rejected into the liquid mass instead of taken up in the solid mass (Vrbka & Jungwirth, 2005). This results in slightly more saline values beneath the sea ice formation.

The freshwater plume and the CDW are too different in density to mix. The water column is baroclinically stable, so there is no initiation for overturning (Dierssen et al., 2002), which results in the strong stratification that we see in the future Ross Sea.

Next to that, with the overall loss of sea ice over the years in the Ross Sea fresh water is added, making the upper layer even less dense. Creating an even stronger separation between this water and the warmer saline water in the layer beneath.

4.6 Explanation rapidity temperature increase

A typical tipping point is associated with a singular catastrophic event (Heinze et al., 2021). In the case of the Ross Sea, the crossing of the Ross Bank might represent this. We think that there is already some exchange between east and west as they are adjacent waters, but now that there is a new established ASC route, the warmer water actually reaches the Western Ross Sea in a great and continuous amount. The Ross Bank formed a barrier for the ASC, the bathymetry is thus quite steering.

Dinniman et al., (2011) also found that in the Ross Sea, bathymetry is primarily determining the locations of the CDW crossing of the shelf break.

4.7 Impact on Ross Ice Shelf

The melting of the Ross Ice Shelf is controlled by ocean mixing and heat transport processes, as observed by Stevens et al., (2020). As is shown by the temperature and salinity cross sections (Figures 8 and 15), the Western Ross Sea is well mixed in the historical situation.

In the future this ocean mixing will decrease (shown in the temperature and salinity analysis) and the heat transport (ASC) pathway will change. The cold cavity underneath the Western Ross Ice Shelf will become a warm cavity and this has consequences for the stability of the shelf. Thompson et al., (2018) categorizes cavities (shelves) into three types: Cold, Dense and Warm (Figure 28), placing the historical Western Ross Sea under 'Dense shelf', because of the AABW formation. Our results show that the future Western Ross Sea will become a 'Warm shelf'.

Similar changes for the Weddell Sea have been found by Daae et al., (2020). Here also a change in the CDW transport, in combination with the freshening of the shelf, was needed for warm water to access the ice shelf and become a 'warm shelf'.

The warm water induces basal melt, which will enhance thinning and calving of the ice shelf (Liu et al., 2015). The same has happened to the Totten Ice Shelf, located in East Antarctica, where a change in ocean heat transport (which was confirmed by observations) induced basal melt (Rintoul et al., 2016).

It has been confirmed, using mooring observations, that mass loss from the Ross ice shelf frontal zone (RIFZ) is a significant fraction of the total Ross ice shelf mass loss (Arzeno et al., 2014). Moreover, this paper confirms the RIFZs' rapid responds to modifications in the Ross Sea upper ocean OHC. With high OHC increases, as EC-Earth3 shows, the Antarctic ice sheet will destabilize. This results in the size reduction of the Antarctic ice sheet (Greene et al., 2022) and eventually, this will contribute to sea level rise (see section 1 and Figure 1).

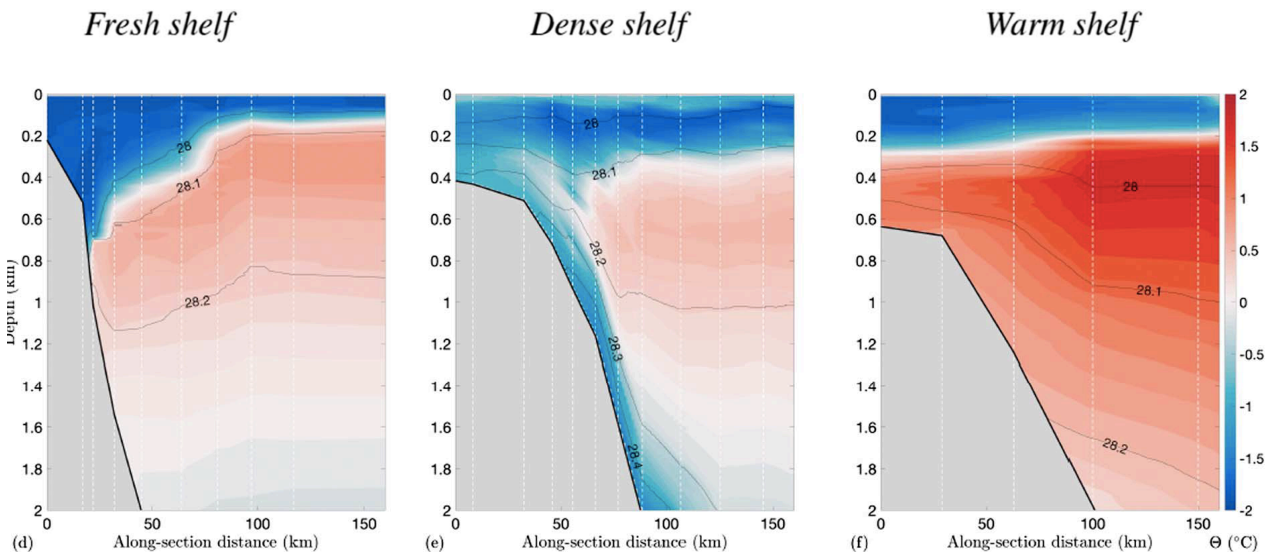

Figure 32. Shelf categorization according to Thompson et al., (2018). Cross shore (cross shelf) cross section for three different types of shelf. The warmer water mass represents the CDW and the cooler water on top is fresher water. The cooler water descending in the 'Dense shelf' frame is the AABW.

4.8 Uncertainties

4.8.1 Quantification

This study is based on following processes visually, it would be convenient to have this accompanied by numbers. A heat budget could be a method for this.
The circulation in the Ross Sea would have to be quantified and the currents must have a temperature assigned to them.
For the heat budget, one could use one inflow in the Eastern Ross Sea and two outflows; (1) before the Ross Bank to the North and (2) after the Ross Bank to the North. The number two outflow quantity should over time match the inflow quantity because in the total transport (ASC) over time shifts from East of the ridge to West of the ridge.
A 4D visualization of the temperature variable would help to assign the temperatures to the waterflows.

4.8.2 Model sensitivity to bathymetry

Bathymetry appears to be very important, however, this research did not assess the sensitivity of EC-Earth3 to it. The irregularity of many shapes in the bathymetry of the Ross Sea hampers the representation in detail in EC-Earth3. The cross-sections through which the in- and outflow is determined should be refined. Felipe et al. (2022) mentions that the coarseness of the UKESM1 model results in a low sensitivity of the flows for bathymetry. A similar assessment could be applied to EC-Earth3, for example by reducing the grid to 0.25 degrees. This comparison between UK ESM and EC-Earth3 could also be expanded to other CMIP6 models, like NorESM2-MM, CAS-ESM2-0 and CMCC-ESM2 (section 1.1).

4.8.3 CDW bias

The CDW in EC-Earth3 is already present on the shelf of the Eastern Ross Sea with an approximate water temperature of 2 degrees C in the historical time frame (1970-1990), though this has not been observed in the real ocean. Schmidtko et al., (2014) combined seven hydrological databases (observational datasets and supplementary materials) with a time frame of 1975 to 2012 and conclude that the shelf bottom water temperature in the Ross Sea is around -1.5 degrees C, so this cannot represent the CDW. EC-Earth3 has thus a bias in this regard and lets the CDW be present on the continental shelf too early.
However, we would still expect the mechanism explained by hypothesis 3 to be present when the Ross Gyre increases in size in the real ocean. Behrens et al., (2016) found the strength of the Ross Gyre to be related to sea ice cover in the future, using the NIWA-UKCA physical climate model (part of CMIP5) and comparing it to other CMIP5 models. Next to that, Felipe et al., (2022) state that the Ross Gyre expansion they found is due to an intensified ocean surface stress curl (westerlies) related to anthropogenic sea ice cover decrease (see also section 1.3.3). As we mentioned in section 1.3.1, atmospheric temperatures increases are already causing melt in Antarctica (Milillo et al., 2022). Therefore, it is not unlikely that this expansion of the Ross Gyre will happen in the real ocean in the future.
Döscher et al., (2022) explains that westerly winds are represented in the model but they are characterized by an underestimation of the winter westerly jet. Further research on this and the relation to the Ross Gyre increase and the CDW bias in EC-Earth3 is needed.

4.9 Future research

4.9.1 Improving meltwater generation in EC-Earth3 by adding basal melt

With respect to section 4.5 and 4.7, it is crucial to add an ice model to EC-Earth3. Currently, the KNMI is working on coupling the model BISICLES (Berkeley Ice Sheet Initiative for CLimate ExtremeS) to EC-Earth3. BISICLES uses adaptive mesh refinement techniques to model the ocean-ice sheet dynamics (Cornford et al., 2013). As the meltwater plume in the results plays a role in the Western Ross Sea OHC in EC-Earth3, the interaction between ice sheet, ice shelf, meltwater and ocean should be further researched. Next to the run-off that currently functions as the meltwater source, basal melt in the cavities should be added.
By adding basal melt, the resulting temperature increase could appear lower (less extreme), as heat will be lost to the melting of the ice shelf. However, the stratification would then probably be enhanced due to additional meltwater, forming the top layer boundary discussed in section 4.5. This is another reason to find out the effect of basal melt in the Ross Sea.

4.9.2 CDW temperature increase

In our results we see the CDW mass increasing in temperature over the years. It should be further researched what causes this temperature increase in EC-Earth3 and if this increase is likely to take place in reality.

4.9.3 AABW formation

With no initiation for overturn in the Western Ross Sea, because the meltwater enhances the stratification (section 4.5.1), we speculate that the sinking of the water, creating the AABW, will decrease or even stop, which is an implication for the global overturning circulation. Apart from that, this has large consequences for ocean biogeochemistry and will warm the abyss of the oceans (Q. Li et al., 2023). Li et al., (2023) did research on abyssal warming with a high-resolution ocean-sea ice coupled model under SSP585. They found that meltwater inflow around Antarctica decreases AABW formation and that abyssal warming will accelerate over the next 30 years. Further research on the Ross Sea overturning cell in EC-Earth3 is needed.

4.9.4 Impact on CO2 sink

Section 1.1.3 explains that ocean temperature is important for primary productivity. Moreau et al., (2019) explains that stratification might lessen primary productivity by reducing the photosynthetic efficiency. Also, with stratification the supply for the needed nutrients will decrease. The stratification in the future Ross Sea might thus lower the local CO2 sequestration. Actual measurements would be necessary to verify this relation in the Ross Sea. However, this is difficult to perform because of the sea ice cover and because the Ross Sea is the worlds' largest protected marine area (Brooks et al., 2020).

4.9.5 Geodynamics

The last suggestion we would like to make is to couple geodynamics in the Ross Sea to EC-Earth3. The Western Ross Sea is an active volcanic area and has a relatively thin lithosphere (Figure 29). Consequently, the predicted heat flux, caused by mantle heat, is high (approximately 110 mW/m2) (Artemieva, 2022). This will probably raise the (Western) Ross Sea ocean temperatures even further.

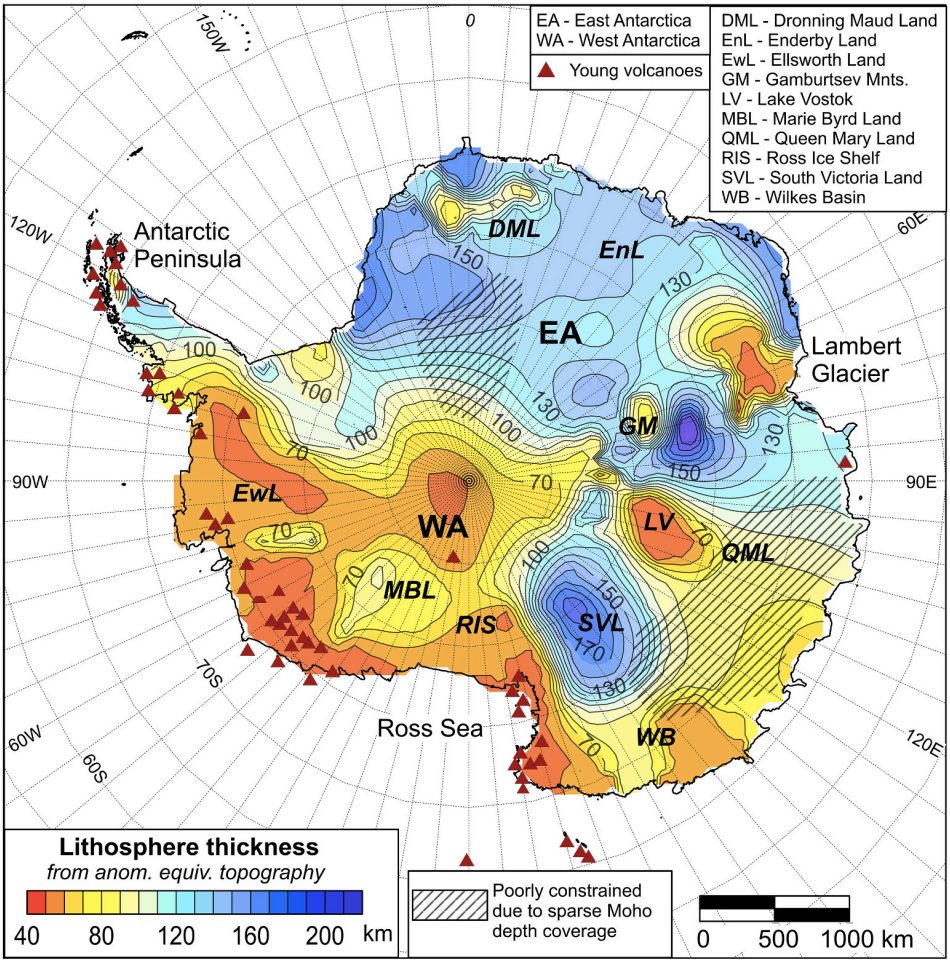

Figure 33. Lithosphere thickness and volcanic activity of Antarctica. The continent around the Ross Sea has a relatively thin lithosphere and a great amount of active volcanos (Artemieva, 2022).

5 Conclusion

Atmospheric warming is not directly responsible for the warming of the Ross Sea at depth; indirectly however, through the disappearance of sea ice, it is. The inflowing ocean temperature of the Western Ross Sea did increase over the years, but not enough to explain the amount of temperature increase at depth. We found that the Ross Gyre did expand and intensified over the years and that this is connected to the pathway and intensity change of the ASC in the Ross Sea. As a result, the transport of water to the West increased over time. Next to that, we found indications for Ekman transport to add to this transport. These two factors ensure a larger amount of warm CDW to enter the Western Ross Sea continuously, with the permanent crossing of the Ross Bank, which is the main explanation for the temperature increase in the Western Ross Sea.

According to literature, it is possible for meltwater to act as a top boundary through which the underlying layer cannot emit its heat. This mechanism is expected to be the reason why the OHC in the Western Ross Sea does not decrease towards Antarctica, together with the fact that the model lacks basal melt.

Thus, the increased temperature in the Western Ross Sea in EC-Earth3 is the result of a change in circulation related to the Ross Gyre, local bathymetry, meltwater presence and model configurations.

This research shows the effect of the Ross Gyre increase on CDW onshore transport and Western Ross Sea temperature. Next to that, it shows the importance of including meltwater perturbations in climate models. Finally, it shows the importance for climate models to be sensitive to the local bathymetry.

Bibliography

Artemieva, I. M. (2022). Antarctica ice sheet basal melting enhanced by high mantle heat. *Earth-Science Reviews*, *226*, 103954. https://doi.org/10.1016/j.earscirev.2022.103954

Arzeno, I. B., Beardsley, R. C., Limeburner, R., Owens, B., Padman, L., Springer, S. R., Stewart, C. L., & Williams, M. J. M. (2014). Ocean variability contributing to basal melt rate near the ice front of Ross Ice Shelf, Antarctica. *Journal of Geophysical Research: Oceans*, *119*, 3868–3882. https://doi.org/10.1002/2014JC009792.Received

Behrens, E., Rickard, G., Morgenstern, O., Martin, T., Osprey, A., & Joshi, M. (2016). Southern Ocean deep convection in global climate models: A driver for variability of subpolar gyres and Drake Passage transport on decadal timescales. *Journal of Geophysical Research: Oceans*, *121*, 3905–3925. https://doi.org/10.1002/2015JC011286

Bigg, G. R., Jickells, T. D., Liss, P. S., & Osborn, T. J. (2003). The role of the oceans in climate. *International Journal of Climatology*, *23*(10), 1127–1159. https://doi.org/10.1002/joc.926

Bronselaer, B., & Zanna, L. (2020). Heat and carbon coupling reveals ocean warming due to circulation changes. *Nature*, *584*(7820), 227–233. https://doi.org/10.1038/s41586-020-2573-5

Brooks, C. M., Crowder, L. B., Österblom, H., & Strong, A. L. (2020). Reaching consensus for conserving the global commons: The case of the Ross Sea, Antarctica. *Conservation Letters*, *13*(1), 1–10. https://doi.org/10.1111/conl.12676

Charrassin, J. B., Hindell, M., Rintoul, S. R., Roquet, F., Sokolov, S., Biuw, M., Costa, D., Boehme, L., Lovell, P., Coleman, R., Timmermann, R., Meijers, A., Meredith, M., Park, Y. H., Bailleul, F., Goebel, M., Tremblay, Y., Bost, C. A., McMahon, C. R., … Guinet, C. (2008). Southern Ocean frontal structure and sea-ice formation rates revealed by elephant seals. *Proceedings of the National Academy of Sciences of the United States of America*, *105*(33), 11634–11639. https://doi.org/10.1073/pnas.0800790105

Cornford, S. L., Martin, D. F., Graves, D. T., Ranken, D. F., Le Brocq, A. M., Gladstone, R. M., Payne, A. J., Ng, E. G., & Lipscomb, W. H. (2013). Adaptive mesh, finite volume modeling of marine ice sheets. *Journal of Computational Physics*, *232*(1), 529–549. https://doi.org/10.1016/j.jcp.2012.08.037

Daae, K., Hattermann, T., Darelius, E., Mueller, R. D., Naughten, K. A., Timmermann, R., & Hellmer, H. H. (2020). Necessary Conditions for Warm Inflow Toward the Filchner Ice Shelf, Weddell Sea. *Geophysical Research Letters*, *47*(22). https://doi.org/10.1029/2020GL089237

Devries, T. (2022). The Ocean Carbon Cycle. *Annual Review of Environment and Resources*, *47*, 317–341. https://doi.org/10.1146/annurev-environ-120920-111307

Dierssen, H. M., Smith, R. C., & Vernet, M. (2002). Glacial meltwater dynamics in coastal waters west of the Antarctic peninsula. *Proceedings of the National Academy of Sciences of the United States of America*, *99*(4), 1790–1795. https://doi.org/10.1073/pnas.032206999

Dinniman, M. S., Klinck, J. M., & Smith, W. O. (2011). A model study of Circumpolar Deep Water on the West Antarctic Peninsula and Ross Sea continental shelves. *Deep-Sea Research Part II: Topical Studies in Oceanography*, *58*(13–16), 1508–1523. https://doi.org/10.1016/j.dsr2.2010.11.013

Döscher, R., Acosta, M., Alessandri, A., Anthoni, P., Arsouze, T., Bergmann, T., Bernadello, R.,

Caron, L., Döscher, R., Acosta, M., Alessandri, A., Anthoni, P., Arneth, A., & Ec-earth, T. (2022). *The EC-Earth3 Earth System Model for the Climate Model Intercomparison Project 6 To cite this version : HAL Id : hal-03451376 The EC-Earth3 Earth system model for the Coupled Model Intercomparison Project 6*.

Dotto, T. S., Naveira Garabato, A., Bacon, S., Tsamados, M., Holland, P. R., Hooley, J., Frajka-Williams, E., Ridout, A., & Meredith, M. P. (2018). Variability of the Ross Gyre, Southern Ocean: Drivers and Responses Revealed by Satellite Altimetry. *Geophysical Research Letters*, *45*(12), 6195–6204. https://doi.org/10.1029/2018GL078607

Dupont, T. K., & Alley, R. B. (2005). Assessment of the importance of ice-shelf buttressing to ice-sheet flow. *Geophysical Research Letters*, *32*(4), 1–4. https://doi.org/10.1029/2004GL022024

Eayrs, C., Li, X., Raphael, M. N., & Holland, D. M. (2021). Rapid decline in Antarctic sea ice in recent years hints at future change. *Nature Geoscience*, *14*(7), 460–464. https://doi.org/10.1038/s41561-021-00768-3

Farooq, U., Rack, W., McDonald, A., & Howell, S. (2023). Representation of sea ice regimes in the Western Ross Sea, Antarctica, based on satellite imagery and AMPS wind data. *Climate Dynamics*, *60*(1–2), 227–238. https://doi.org/10.1007/s00382-022-06319-9

Felipe, G., Holland, P. R., Siahaan, A., & Young, E. (2022). *Projected West Antarctic ocean warming caused by an expansion of the Ross Gyre*. 1–22.

Fox-Kemper, B., Hewitt, H., Xiao, C., Aðalgeirsdóttir, G., Drijfhout, S., Edwards, T., Golledge, N., Hemer, M., Kopp, R., Krinner, G., Mix, A., Notz, D., Nowiciki, S., Nurhati, I., Ruiz, J., Sallée, J., Slangen, A., & Yu, Y. (2021). Chapter 9: Ocean, Cryosphere and Sea Level Change. In *Climate Change 2021: The Physical Science Basis. Contribution of Working Group I to the Sixth Assessment Report of the Intergovernmental Panel on Climate Change* (Issue August). https://doi.org/10.1017/9781009157896.011.1212

Gille, S. T., McKee, D. C., & Martinson, D. G. (2016). Temporal changes in the Antarctic circumpolar current: Implications for the Antarctic continental shelves. *Oceanography*, *29*(4), 96–105. https://doi.org/10.5670/oceanog.2016.102

Gouretski, V. (1999). The Large-Scale Thermohaline Structure of the Ross Gyre. In *Oceanography of the Ross Sea Antarctica* (pp. 77–100). https://doi.org/10.1007/978-88-470-2250-8_6

Gouretski, Viktor. (1999). Oceanography of the Ross Sea Antarctica. In *Oceanography of the Ross Sea Antarctica* (Issue January 1999). https://doi.org/10.1007/978-88-470-2250-8

Greene, C. A., Gardner, A. S., Schlegel, N. J., & Fraser, A. D. (2022). Antarctic calving loss rivals ice-shelf thinning. *Nature*, *609*(7929), 948–953. https://doi.org/10.1038/s41586-022-05037-w

Gulev, S. K., Thorne, P. W., Ahn, J., Dentener, F. J., Domingues, C. M., Gerland, S., Gong, D., Kaufman, D. S., Nnamchi, H. C., Quaas, J., Rivera, J. A., Sathyendranath, S., Smith, S. L., Trewin, B., Schuckmann, K. von, & Vose, R. S. (2021). Chapter 2: The Changing State of the Climate. In *Climate Change 2021: The Physical Science Basis. Contribution of Working Group I to the Sixth Assessment Report of the Intergovernmental Panel on Climate Change*. Climate Change 2021: The Physical Science Basis. Contribution of Working Group I to the Sixth Assessment Report of the Intergovernmental Panel on Climate Change. https://doi.org/10.1017/9781009157896.004.288

Heinze, C., Blenckner, T., Martins, H., Rusiecka, D., Döscher, R., Gehlen, M., Gruber, N., Holland, E., Hov, Ø., Joos, F., Matthews, J. B. R., Rødven, R., & Wilson, S. (2021). The quiet crossing of ocean tipping points. *Proceedings of the National Academy of Sciences*

of the United States of America, *118*(9), 1–9. https://doi.org/10.1073/pnas.2008478118
Hersbach, H., Bell, B., Berrisford, P., Hirahara, S., Horányi, A., Muñoz-Sabater, J., Nicolas, J., Peubey, C., Radu, R., Schepers, D., Simmons, A., Soci, C., Abdalla, S., Abellan, X., Balsamo, G., Bechtold, P., Biavati, G., Bidlot, J., Bonavita, M., … Thépaut, J. N. (2020). The ERA5 global reanalysis. *Quarterly Journal of the Royal Meteorological Society*, *146*(730), 1999–2049. https://doi.org/10.1002/qj.3803
Holland, P. R., Bracegirdle, T. J., Dutrieux, P., Jenkins, A., & Steig, E. J. (2019). West Antarctic ice loss influenced by internal climate variability and anthropogenic forcing. *Nature Geoscience*, *12*(9), 718–724. https://doi.org/10.1038/s41561-019-0420-9
Hyder, P., Edwards, J. M., Allan, R. P., Hewitt, H. T., Bracegirdle, T. J., Gregory, J. M., Wood, R. A., Meijers, A. J. S., Mulcahy, J., Field, P., Furtado, K., Bodas-Salcedo, A., Williams, K. D., Copsey, D., Josey, S. A., Liu, C., Roberts, C. D., Sanchez, C., Ridley, J., … Belcher, S. E. (2018). Critical Southern Ocean climate model biases traced to atmospheric model cloud errors. *Nature Communications*, *9*(1). https://doi.org/10.1038/s41467-018-05634-2
Ingrosso, G., Giani, M., Kralj, M., Comici, C., Rivaro, P., Budillon, G., Castagno, P., Zoccarato, L., & Celussi, M. (2022). Physical and biological controls on anthropogenic CO2 sink of the Ross Sea. *Frontiers in Marine Science*, *9*(September), 1–19. https://doi.org/10.3389/fmars.2022.954059
Kwiatkowski, L., Torres, O., Bopp, L., Aumont, O., Chamberlain, M., R. Christian, J., P. Dunne, J., Gehlen, M., Ilyina, T., G. John, J., Lenton, A., Li, H., S. Lovenduski, N., C. Orr, J., Palmieri, J., Santana-Falcón, Y., Schwinger, J., Séférian, R., A. Stock, C., … Ziehn, T. (2020). Twenty-first century ocean warming, acidification, deoxygenation, and upper-ocean nutrient and primary production decline from CMIP6 model projections. *Biogeosciences*, *17*(13), 3439–3470. https://doi.org/10.5194/bg-17-3439-2020
Lambert, E., Le Bars, D., van der Linden, E., Jüling, A., & Drijfhout, S. (n.d.). Quantifying the feedback between Antarctic freshwater release and the Southern Ocean Warming. *In Preparation*.
Lecomte, O., Goosse, H., Fichefet, T., De Lavergne, C., Barthélemy, A., & Zunz, V. (2017). Vertical ocean heat redistribution sustaining sea-ice concentration trends in the Ross Sea. *Nature Communications*, *8*(1). https://doi.org/10.1038/s41467-017-00347-4
Li, Q., England, M. H., Hogg, A. M., Rintoul, S. R., & Morrison, A. K. (2023). Supplementary to Abyssal ocean overturning slowdown and warming driven by Antarctic meltwater. *Nature*, *615*(March 2022). https://doi.org/10.1038/s41586-023-05762-w
Li, X., Cai, W., Meehl, G. A., Chen, D., Yuan, X., Raphael, M., Holland, D. M., Ding, Q., Fogt, R. L., Markle, B. R., Wang, G., Bromwich, D. H., Turner, J., Xie, S. P., Steig, E. J., Gille, S. T., Xiao, C., Wu, B., Lazzara, M. A., … Song, C. (2021). Tropical teleconnection impacts on Antarctic climate changes. *Nature Reviews Earth and Environment*, *2*(10), 680–698. https://doi.org/10.1038/s43017-021-00204-5
Liu, Y., Moore, J. C., Cheng, X., Gladstone, R. M., Bassis, J. N., Liu, H., Wen, J., & Hui, F. (2015). Ocean-driven thinning enhances iceberg calving and retreat of Antarctic ice shelves. *Proceedings of the National Academy of Sciences of the United States of America*, *112*(11), 3263–3268. https://doi.org/10.1073/pnas.1415137112
Meinshausen, M., Vogel, E., Nauels, A., Lorbacher, K., Meinshausen, N., Etheridge, D. M., Fraser, P. J., Montzka, S. A., Rayner, P. J., Trudinger, C. M., Krummel, P. B., Beyerle, U., Canadell, J. G., Daniel, J. S., Enting, I. G., Law, R. M., Lunder, C. R., O'Doherty, S., Prinn, R. G., … Weiss, R. (2017). Historical greenhouse gas concentrations for climate

modelling (CMIP6). *Geoscientific Model Development*, *10*(5), 2057–2116. https://doi.org/10.5194/gmd-10-2057-2017

Meredith, M., Sommerkorn, M., Cassotta, S., Derksen, C., Ekaykin, A., Hollowed, A., Kofinas, G., Mackintosh, A., Melbourne-Thomas, J., Muelbert, M. M. ., Ottersen, G., Preitchard, H., & Schuur, E. A. G. (2019). Polar regions. In H.-O Pörtner, et al. (2021). *IPCC Special Report on the Ocean and Cryosphere in a Changing Climate*, 203–320.

Milillo, P., Rignot, E., Rizzoli, P., Scheuchl, B., Mouginot, J., Bueso-Bello, J. L., Prats-Iraola, P., & Dini, L. (2022). Rapid glacier retreat rates observed in West Antarctica. *Nature Geoscience*, *15*(1), 48–53. https://doi.org/10.1038/s41561-021-00877-z

Moreau, S., Lannuzel, D., Janssens, J., Arroyo, M. C., Corkill, M., Cougnon, E., Genovese, C., Legresy, B., Lenton, A., Puigcorbé, V., Ratnarajah, L., Rintoul, S., Roca-Martí, M., Rosenberg, M., Shadwick, E. H., Silvano, A., Strutton, P. G., & Tilbrook, B. (2019). Sea Ice Meltwater and Circumpolar Deep Water Drive Contrasting Productivity in Three Antarctic Polynyas. *Journal of Geophysical Research: Oceans*, *124*(5), 2943–2968. https://doi.org/10.1029/2019JC015071

National Academies of Science Engineering and Medicine. (2015). *A Strategic Vision for NSF Investments in Antarctic and Southern Ocean Research*. The National Academies Press.

Naughten, K. A., Holland, P. R., Dutrieux, P., Kimura, S., Bett, D. T., & Jenkins, A. (2022). Simulated Twentieth-Century Ocean Warming in the Amundsen Sea, West Antarctica. *Geophysical Research Letters*, *49*(5). https://doi.org/10.1029/2021GL094566

O'Neill, B. C., Tebaldi, C., Van Vuuren, D. P., Eyring, V., Friedlingstein, P., Hurtt, G., Knutti, R., Kriegler, E., Lamarque, J. F., Lowe, J., Meehl, G. A., Moss, R., Riahi, K., & Sanderson, B. M. (2016). The Scenario Model Intercomparison Project (ScenarioMIP) for CMIP6. *Geoscientific Model Development*, *9*(9), 3461–3482. https://doi.org/10.5194/gmd-9-3461-2016

Orsi, A. H., & Wiederwohl, C. L. (2009). A recount of Ross Sea waters. *Deep-Sea Research Part II: Topical Studies in Oceanography*, *56*(13–14), 778–795. https://doi.org/10.1016/j.dsr2.2008.10.033

Pörtner, H.-O., Roberts, D. C., Poloczanska, E. S., Mintenbeck, K., Tignor, M., Alegría, A., Craig, M., Langsdorf, S., Löschke, S., Möller, V., Okem, A., & (eds.). (2022). Summary for Policymakers. In *Climate Change 2022: Impacts, Adaptation and Vulnerability. Contribution of Working Group II to the Sixth Assessment Report of the Intergovernmental Panel on Climate Change [[H.-O. Pörtner, D.C. Roberts, M. Tignor, E.S. Poloczanska, K. Mintenbeck, A. Ale*. https://doi.org/10.1017/CBO9781139177245.003

Rignot, E., Jacobs, S., Mouginot, J., & Scheuchl, B. (2013). Ice-shelf melting around antarctica. *Science*, *341*(6143), 266–270. https://doi.org/10.1126/science.1235798

Rintoul, S. R., Silvano, A., Pena-Molino, B., Van Wijk, E., Rosenberg, M., Greenbaum, J. S., & Blankenship, D. D. (2016). Ocean heat drives rapid basal melt of the totten ice shelf. *Science Advances*, *2*(12), 1–6. https://doi.org/10.1126/sciadv.1601610

Riser, S. C., Freeland, H. J., Roemmich, D., Wijffels, S., Troisi, A., Belbéoch, M., Gilbert, D., Xu, J., Pouliquen, S., Thresher, A., Le Traon, P. Y., Maze, G., Klein, B., Ravichandran, M., Grant, F., Poulain, P. M., Suga, T., Lim, B., Sterl, A., … Jayne, S. R. (2016). Fifteen years of ocean observations with the global Argo array. *Nature Climate Change*, *6*(2), 145–153. https://doi.org/10.1038/nclimate2872

Schmidtko, S., Heywood, K. J., Thompson, A. F., & Aoki, S. (2014). Multidecadal warming of Antarctic waters. *Science*, *346*(6214), 1227–1231.

https://doi.org/10.1126/science.1256117
Smith, W. O., Ainley, D. G., Arrigo, K. R., & Dinniman, M. S. (2014). The oceanography and ecology of the ross sea. *Annual Review of Marine Science*, *6*, 469–487. https://doi.org/10.1146/annurev-marine-010213-135114
Stevens, C., Hulbe, C., Brewer, M., Stewart, C., Robinson, N., Ohneiser, C., & Jendersie, S. (2020). Ocean mixing and heat transport processes observed under the Ross Ice Shelf control its basal melting. *Proceedings of the National Academy of Sciences of the United States of America*, *117*(29), 16799–16804. https://doi.org/10.1073/pnas.1910760117
Talley, L. D. (2013). Closure of the global overturning circulation through the Indian, Pacific and Southern Oceans: schematics and transports. *Journal of Chemical Information and Modeling*, *53*(9), 1689–1699.
Thompson, A. F., Stewart, A. L., Spence, P., & Heywood, K. J. (2018). The Antarctic Slope Current in a Changing Climate. *Reviews of Geophysics*, *56*(4), 741–770. https://doi.org/10.1029/2018RG000624
Thorpe, S. A. (2005). *The Turbulent Ocean*. Cambridge Univeristy Press.
Toggweiler, J. R., & Key, R. M. (2001). Thermohaline Circulation. *Encyclopedia of Ocean Sciences*, 2941–2947. https://doi.org/10.1006/rwos.2001.0111
Vrbka, L., & Jungwirth, P. (2005). Brine rejection from freezing salt solutions: A molecular dynamics study. *Physical Review Letters*, *95*(14). https://doi.org/10.1103/PhysRevLett.95.148501
Wyser, K., Van Noije, T., Yang, S., Von Hardenberg, J., O'Donnell, D., & Döscher, R. (2020). On the increased climate sensitivity in the EC-Earth model from CMIP5 to CMIP6. *Geoscientific Model Development*, *13*(8), 3465–3474. https://doi.org/10.5194/gmd-13-3465-2020

Appendix 1

Forcing datasets as summarized by Dösher et al. (2022)

Table 13. CMIP6 forcing datasets used by EC-Earth3 and EC-Earth3-Veg for DECK (diagnostic, evaluation, and characterization of klima) and historical experiments. All datasets are available from https://esgf-node.llnl.gov/search/input4mips/ (last access: 18 March 2022). A more detailed description of the CMIP6 forcing datasets is available at http://goo.gl/r8up31 (last access: 18 March 2022).

Forcing dataset	Version	Further info	Comments
Greenhouse gas concentration	1.2.0	Meinshausen et al. (2017)	
Stratospheric aerosols	3.0.0	Thomason et al. (2018)	
Ozone volume mixing ratio	1.0	http://blogs.reading.ac.uk/ccmi/forcing-databases-in-support-of-cmip6/, (last access: 18 March 2022; Hegglin et al., 2021)	
Solar	3.2	Matthes et al. (2017)	
Aerosol optical properties and relative change in cloud droplet number concentration	MACv2-SP	Stevens et al. (2017)	
Land use	v2.1 (h)istoric and (f)uture	Hurtt et al. (2019a, b, 2020)	Used only in combination with dynamic vegetation model
Nitrogen deposition	v2.0	http://blogs.reading.ac.uk/ccmi/forcing-databases-in-support-of-cmip6/ (last access: 18 March 2022; Hegglin et al., 2021)	Used only in combination with dynamic vegetation model